

Heavy Ion and cosmic ray generators

Klaus Werner

Contents

I Introduction	3
II Theoretical concepts	34
III Model overview	77
IV Multiple scattering in EPOS	92
V Collectivity in EPOS	136
VI Flow in small systems	160
VII Recent developments	176

I Introduction

Before 2010:

Proton-proton scattering:
elementary, understood in terms of pQCD

Heavy ion collisions:
Collective effects, formation of a (flowing)
quark-gluon-plasma, macroscopic description

Since 2010: Incredibly interesting and unexpected pp and pPb results at the LHC (**collective effect also in pp?**)

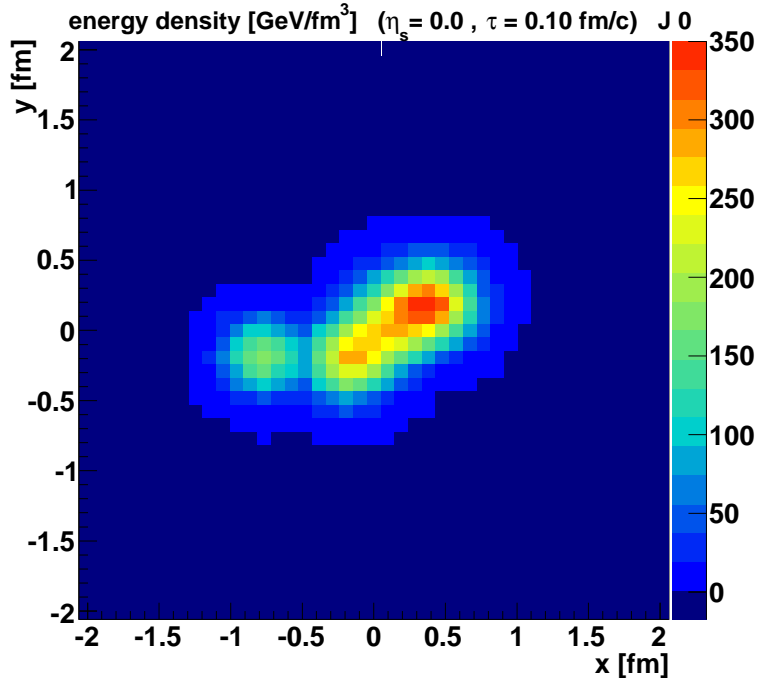
Collective effects means

- **Primary interactions at $t = 0$**
- **Secondary interactions**
formation of “matter” which expands collectively, like a fluid

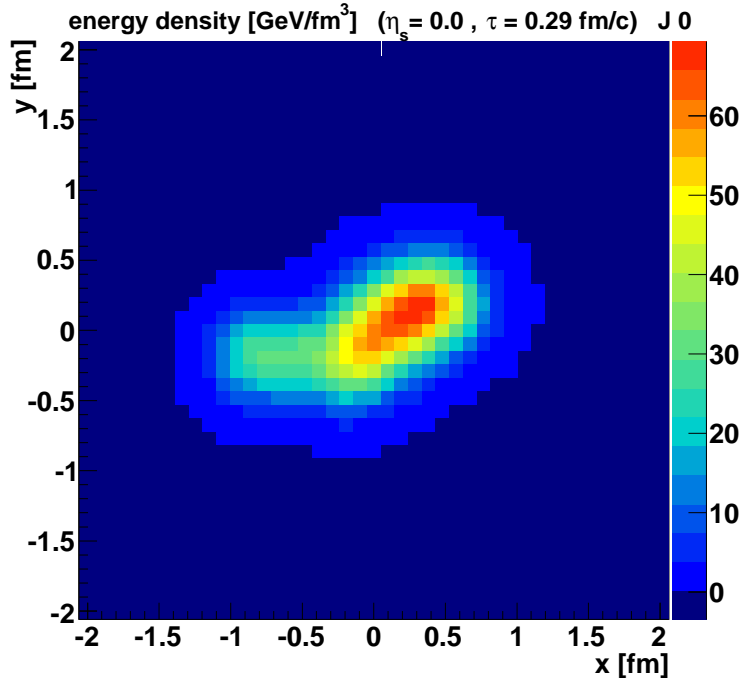
In the following:

An example of a EPOS simulation of expanding matter in pp scattering

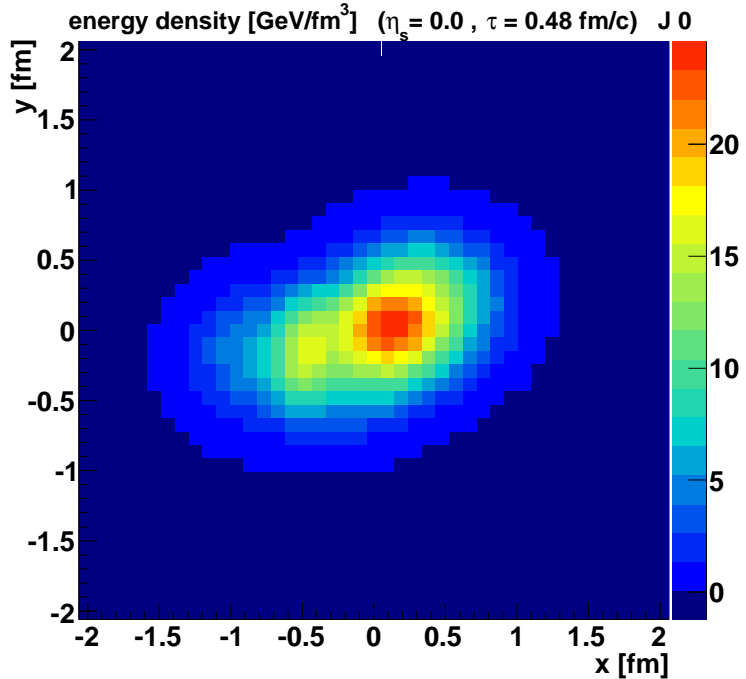
pp @ 7TeV EPOS 3.119



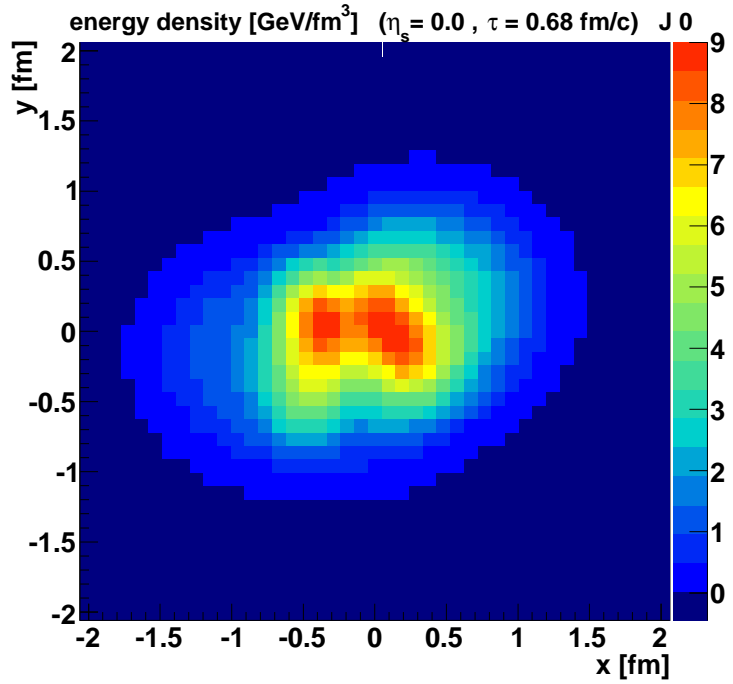
pp @ 7TeV EPOS 3.119



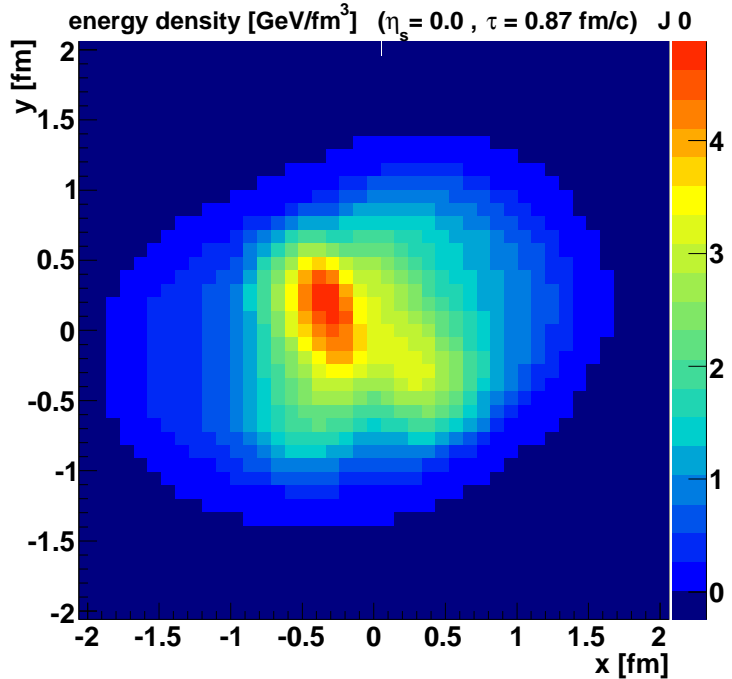
pp @ 7TeV EPOS 3.119



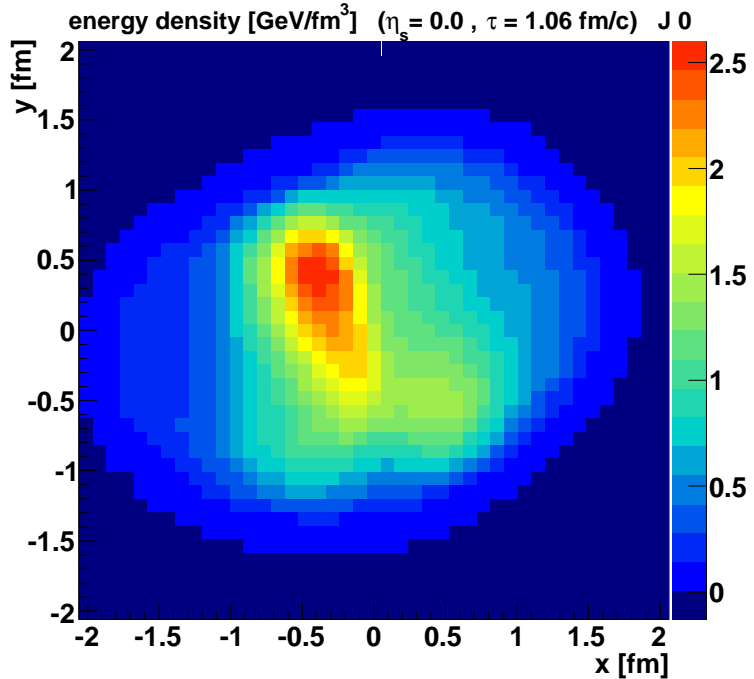
pp @ 7TeV EPOS 3.119



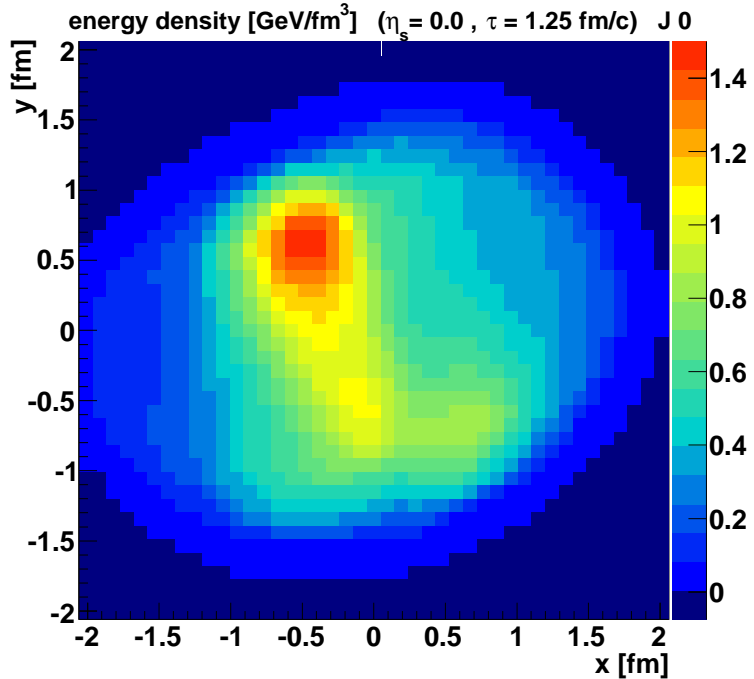
pp @ 7TeV EPOS 3.119



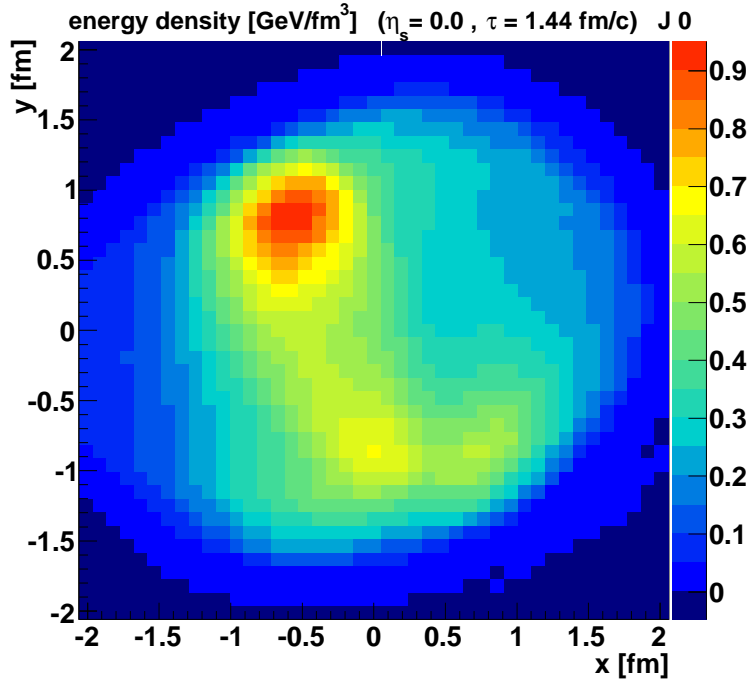
pp @ 7TeV EPOS 3.119



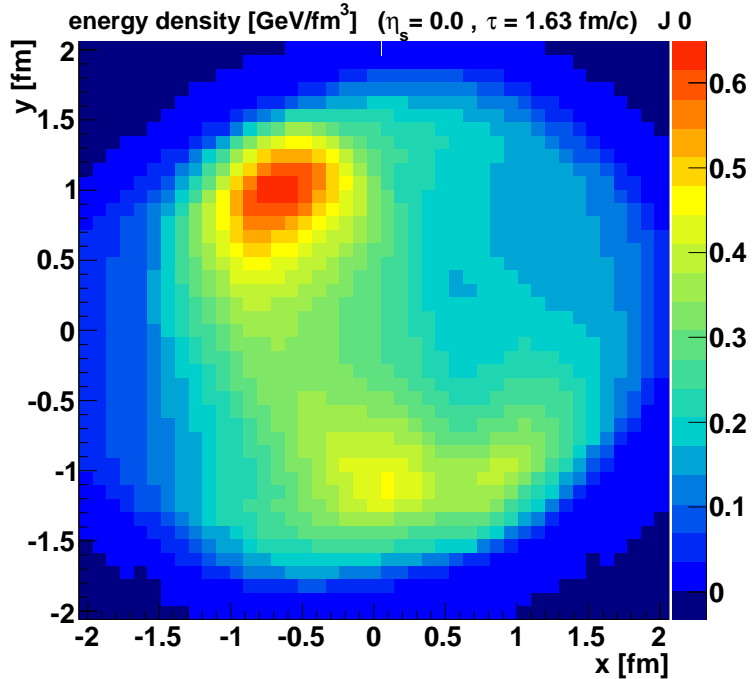
pp @ 7TeV EPOS 3.119



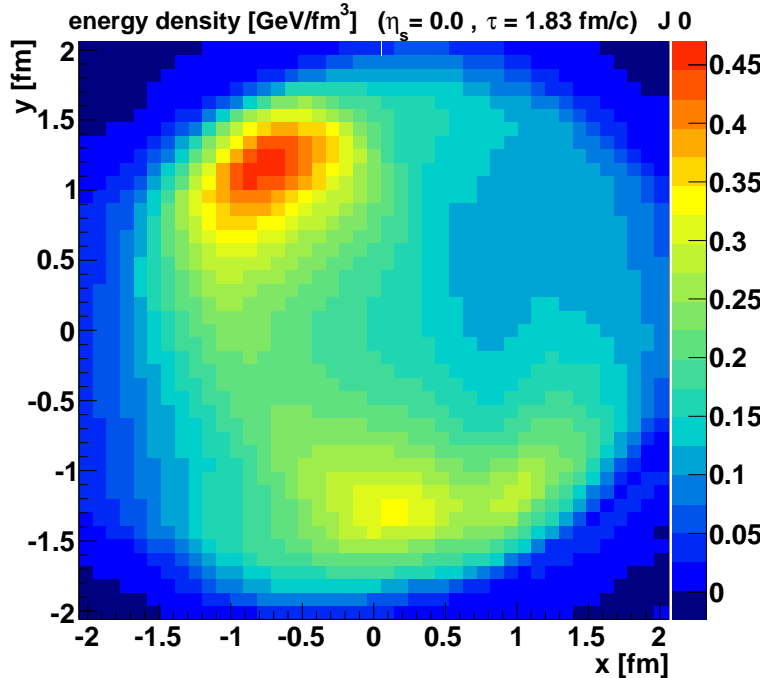
pp @ 7TeV EPOS 3.119



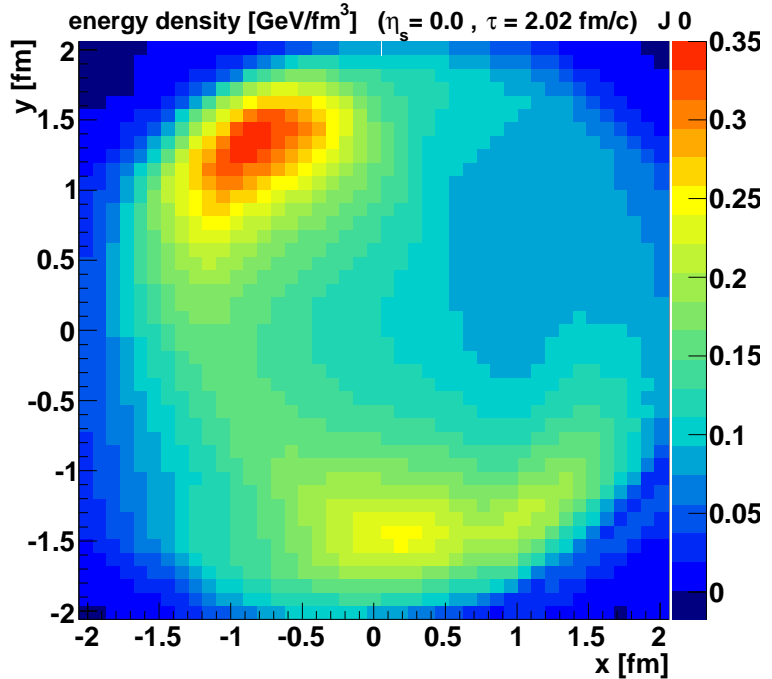
pp @ 7TeV EPOS 3.119



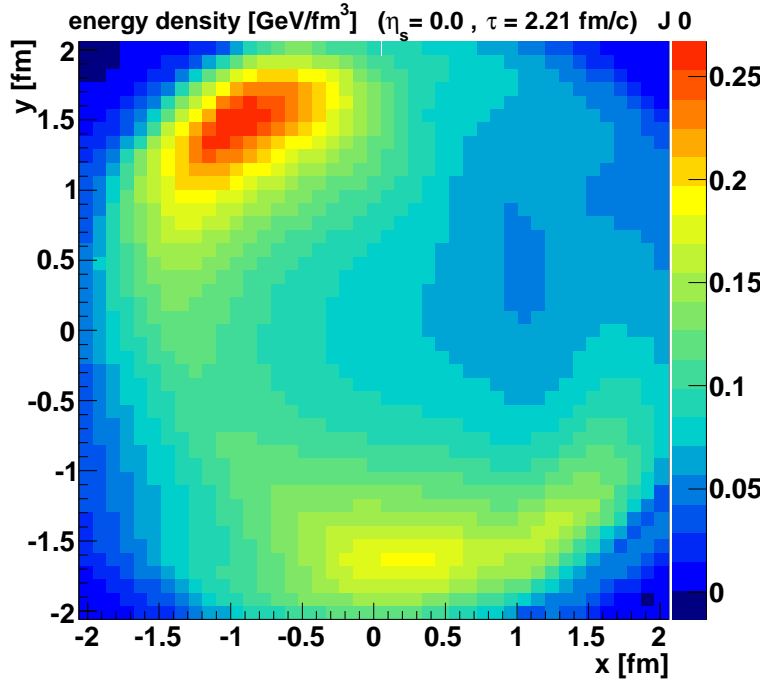
pp @ 7TeV EPOS 3.119



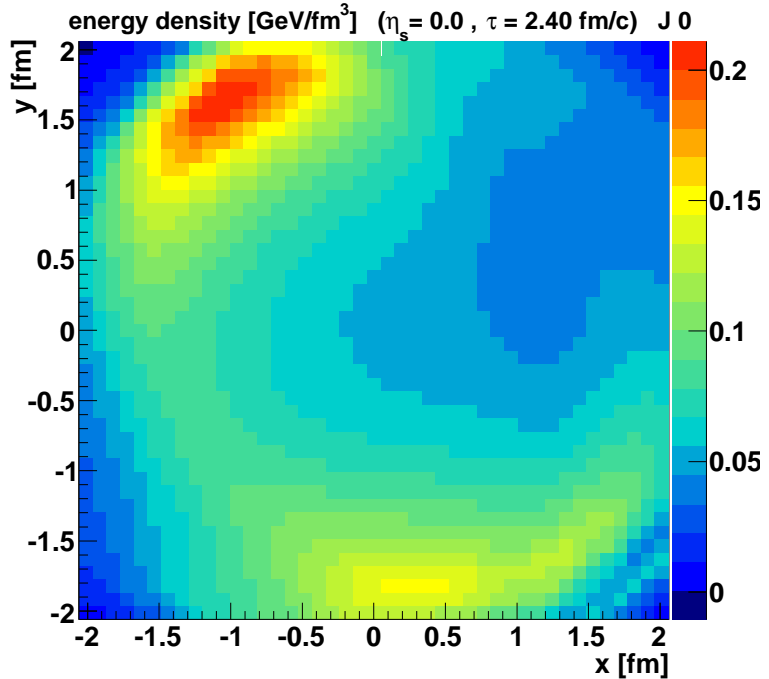
pp @ 7TeV EPOS 3.119



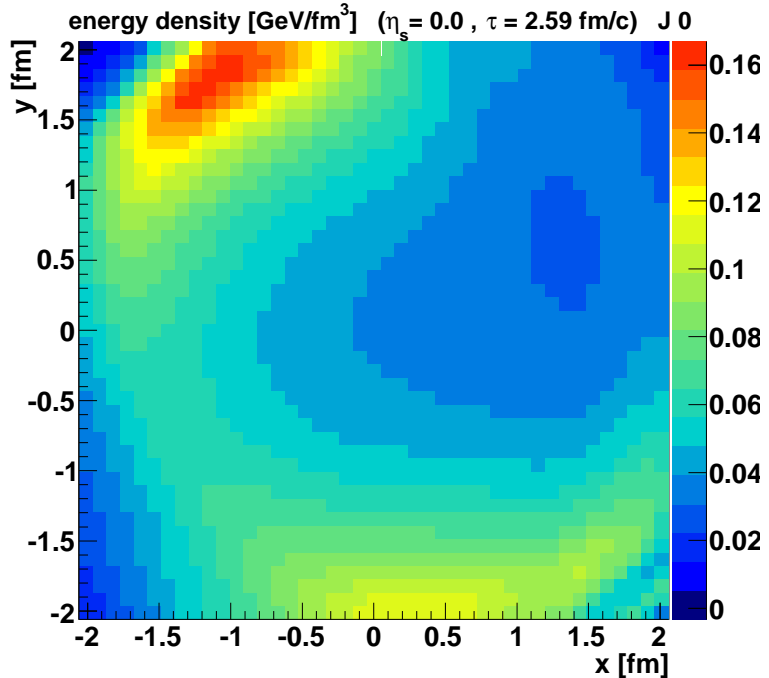
pp @ 7TeV EPOS 3.119



pp @ 7TeV EPOS 3.119

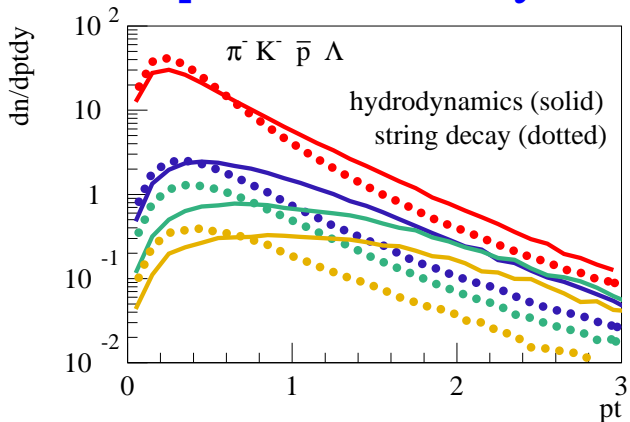


pp @ 7TeV EPOS 3.119



Radial flow visible in particle distributions

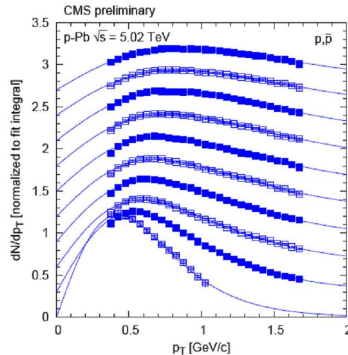
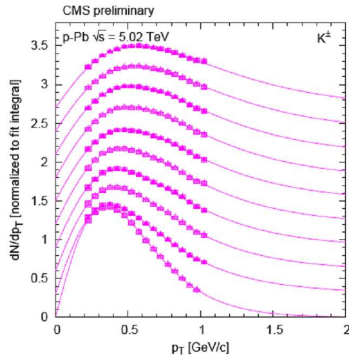
Particle spectra affected by radial flow



=> mass ordering of $\langle p_t \rangle$, lambda/K increase

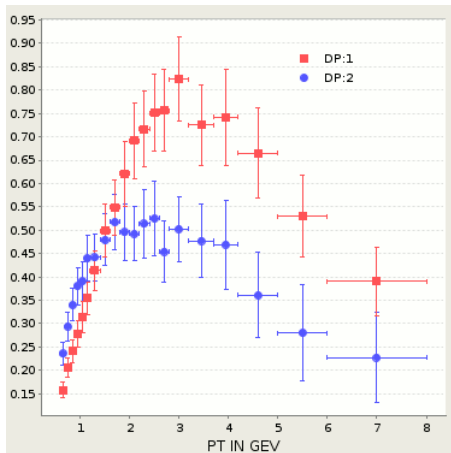
pPb at 5TeV

CMS, arXiv:1307.3442

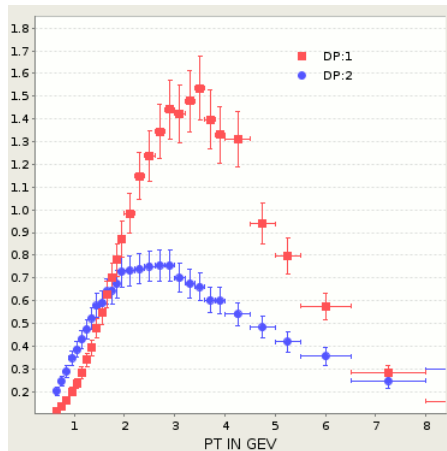


Strong variation of shape with multiplicity
for kaon and even more for proton pt spectra
(flow like)

Λ/K_s versus p_T (high compared to low multiplicity) in pPb (left) similar to PbPb (right)



ALICE (2013) arXiv:1307.6796



ALICE (2013) arXiv:1307.5530

Phys. Rev. Lett. 111, 222301 (2013)

In AA: partially due to flow

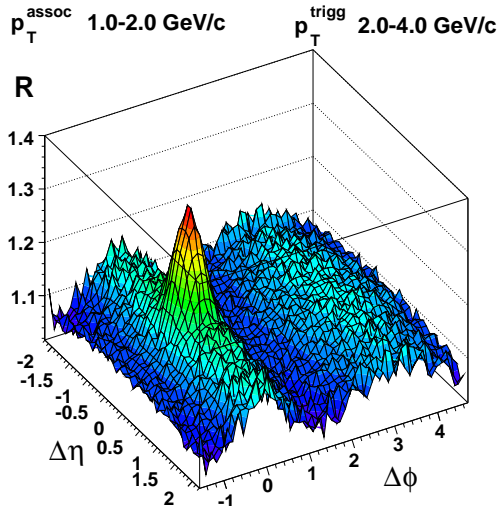
Ridges & flow harmonics

Ridges appear in

$$R = \frac{1}{N_{\text{trigg}}} \frac{dn}{d\Delta\phi\Delta\eta}$$

**due to initial
azimuthal
anisotropies**

(longitudinally
invariant)

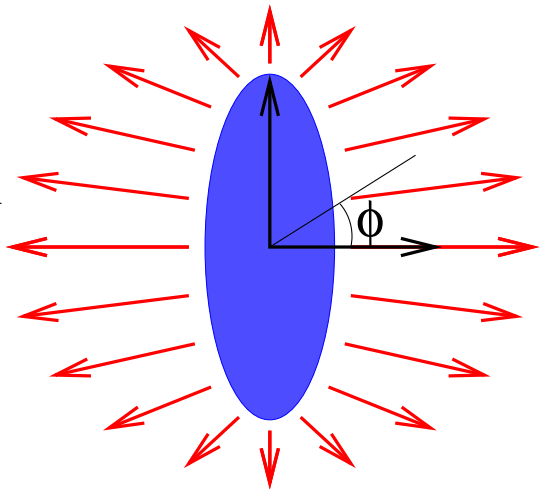


EPOS3.074

**Initial “elliptical”
matter distribution:**

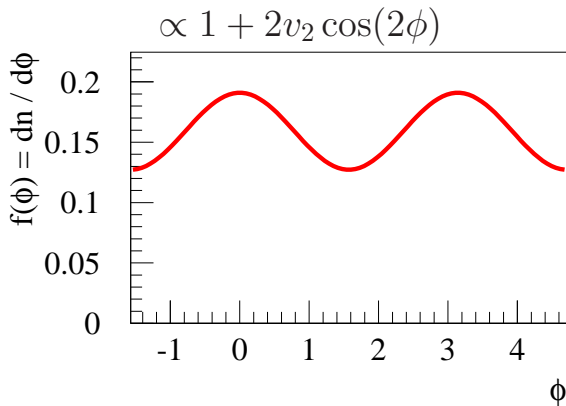
Preferred expansion
along $\phi = 0$
and $\phi = \pi$

η_s -invariance
same form at any η_s
 $\eta_s = \frac{1}{2} \ln \frac{t+z}{t-z}$



Particle
distribution:
Preferred
directions

$$\phi = 0 \text{ and } \phi = \pi$$



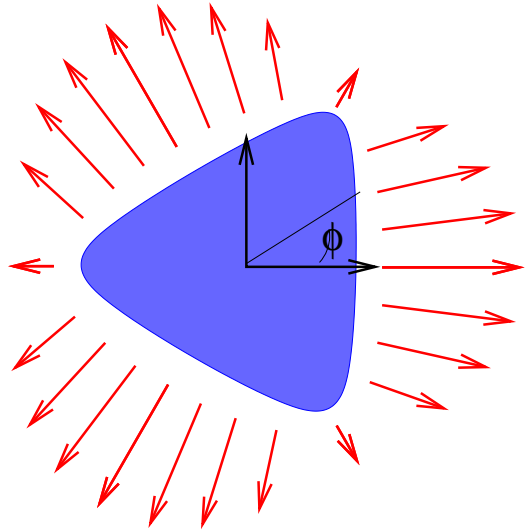
Dihadrons:

preferred $\Delta\phi = 0$ and $\Delta\phi = \pi$ (even for big $\Delta\eta$)

**Initial “triangular”
matter distribu-
tion:**

Preferred expansion
along $\phi = 0$, $\phi = \frac{2}{3}\pi$,
and $\phi = \frac{4}{3}\pi$

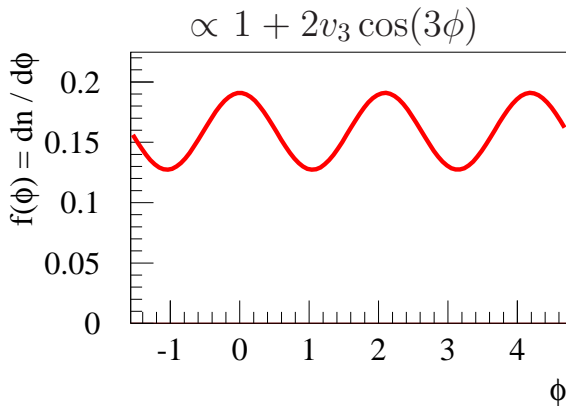
η_s -invariance



Particle
distribution:
Preferred
directions

$$\phi = 0, \phi = \frac{2}{3}\pi,$$

and $\phi = \frac{4}{3}\pi$



Dihadrons:

preferred $\Delta\phi = 0$, and $\Delta\phi = \frac{2}{3}\pi$, and $\Delta\phi = \frac{4}{3}\pi$
(even for large $\Delta\eta$)

In general, superposition of several eccentricities ε_n ,

$$\varepsilon_n e^{in\psi_n^{PP}} = -\frac{\int dx dy r^2 e^{in\phi} e(x, y)}{\int dx dy r^2 e(x, y)}$$

Particle distribution characterized by harmonic flow coefficients

$$v_n e^{in\psi_n^{EP}} = \int d\phi e^{in\phi} f(\phi)$$

At $\phi = 0$:

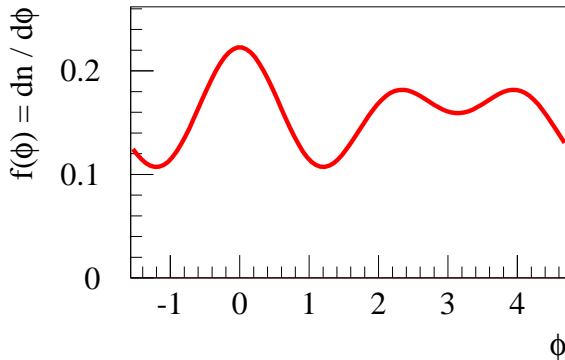
The **ridge**

(extended in η)

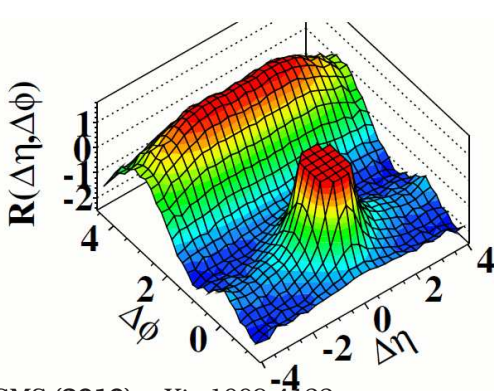
Awayside peak
may originate
from jets, not
the ridge (for
large $\Delta\eta$)

Here, v_2 and v_3 non-zero

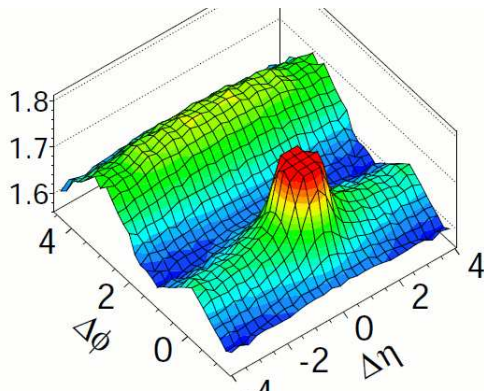
$$\propto 1 + 2v_2 \cos(2\phi) + 2v_3 \cos(3\phi)$$



**CMS: Ridges (in dihadron correlation functions)
also seen in pp (left) and pPb (right)**



CMS (2010) arXiv:1009.4122
JHEP 1009:091,2010



CMS (2012) arXiv:1210.5482
Phys. Lett. B 718 (2013) 795

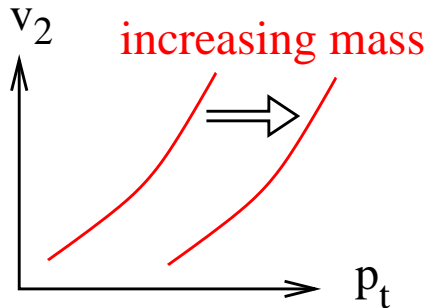
Looks like flow !

Flow harmonics, identified particles

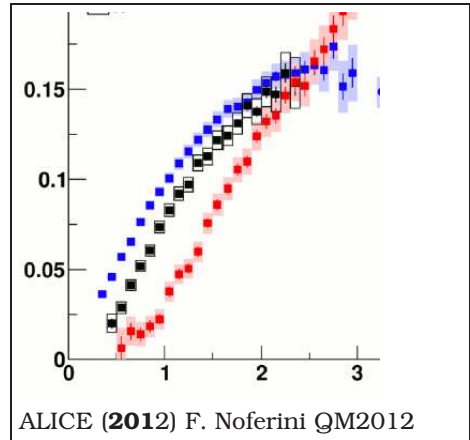
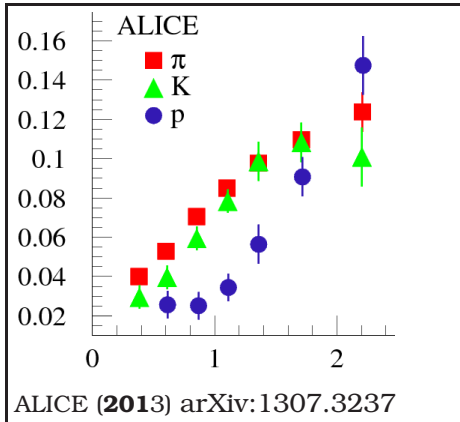
Flow shifts particles to higher p_t

Effect increases with mass

Also true for v_2
vs p_t



ALICE: v_2 versus p_T : mass splitting (π , K , p) in pPb (left) similar to PbPb (right)



Typical flow result!

So : “Flow-like phenomena” are also seen in pp and pA, therefore:

Heavy ion approach

**= primary scattering
+ subsequent fluid evolution**

becomes interesting for pp and pA

II Theoretical concepts

concerning primary interactions

providing initial conditions
for secondary interactions

Poles and branch cuts

Even functions $f(x)$ of a **real variable** x may need to be **continued into the complex plane**, to understand their properties.

Example
$$f(x) = \sum_{n=0}^{\infty} a_n x^n = \sum_{n=0}^{\infty} \left(\frac{x}{2i}\right)^n .$$

The radius of convergence is

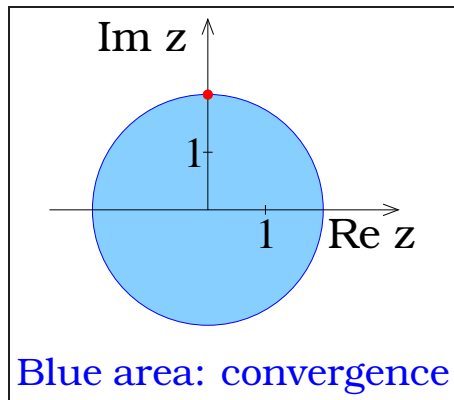
$$\rho = \lim_{n \rightarrow \infty} |a_n|^{-1/n} = 2$$

Which is obvious, since f considered as function of a complex variable z , writes

$$f(z) = \frac{1}{1 - z/(2i)}$$

having a **pole** at $z = 2i$,

whereas $f(x)$ has no singularity (for $x \in \mathbb{R}$)



Branch cuts

An example: The logarithm.

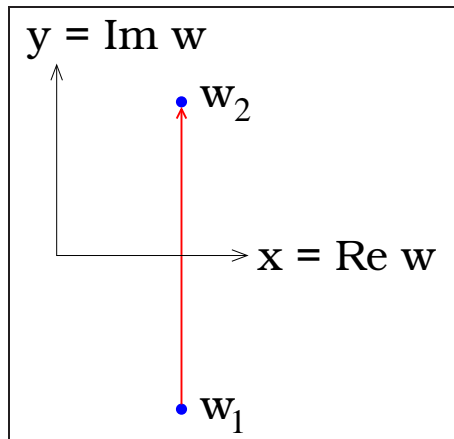
The exponential function defines a mapping M

$$M : \begin{array}{l} \mathbb{C} \rightarrow \mathbb{C} \\ w \rightarrow z = \exp(w) \end{array}$$

which is well defined in the whole complex plane.

Consider $w = x + iy$, with x fixed and y going from $-\pi$ to π .

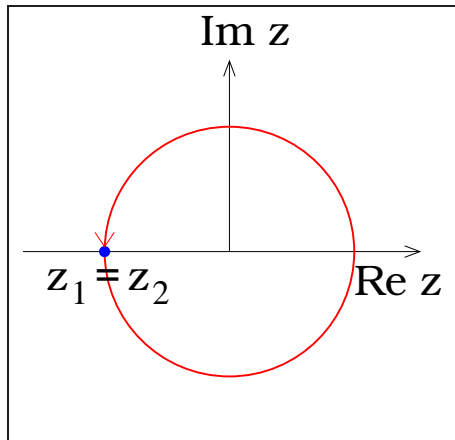
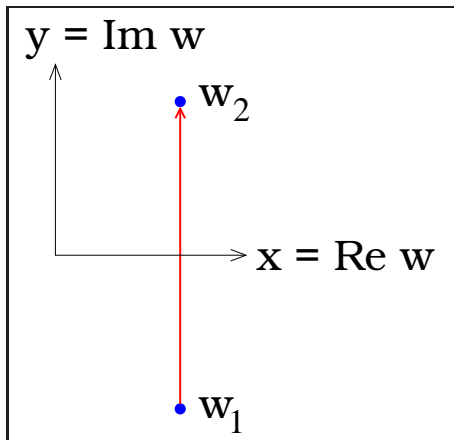
(Trajectory γ going from $w_1 = x - i\pi$ to $w_2 = x + i\pi$)



The mapped trajectory $\gamma' = M(\gamma)$ is given as

$$z = \exp(w) = \exp(x) \exp(iy)$$

=> A circle with start and end point $z_1 = z_2 = -e^x$

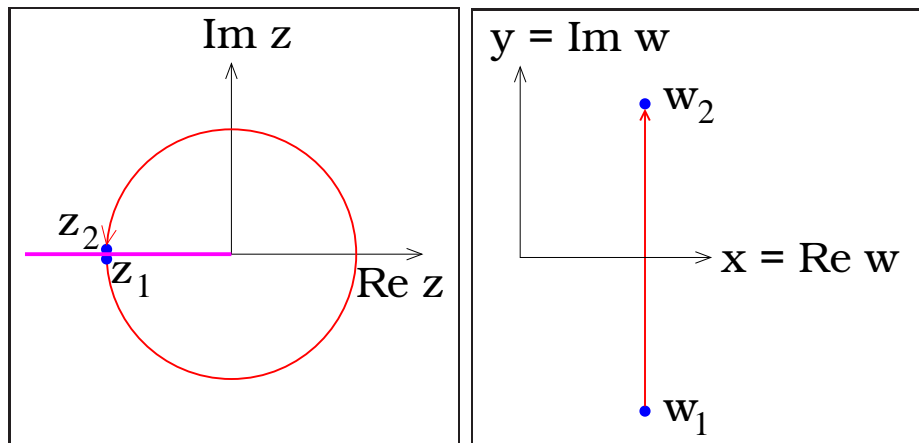


Doing the inverse mapping

$$M^{-1} : z \rightarrow w = \log(z),$$

we get for $z_1 = z_2$ two different values w_1 and w_2 !!

One has to define \log in $\mathbb{C} - \mathbb{R}_{\leq 0}$ (branch).
The negative real axis is called branch cut.



The discontinuity at $z = -e^x$:

$$\log(z + i\epsilon) - \log(z - i\epsilon) = 2\pi i$$

Cut diagrams

The scattering operator \hat{S} is defined via

$$|\psi(t = +\infty)\rangle = \hat{S} |\psi(t = -\infty)\rangle$$

Unitarity relation $\hat{S}^\dagger \hat{S} = 1$ gives

$$\begin{aligned} 1 &= \langle i | \hat{S}^\dagger \hat{S} | i \rangle \\ &= \sum_f \langle i | \hat{S}^\dagger | f \rangle \langle f | \hat{S} | i \rangle \\ &= \sum_f \langle f | \hat{S} | i \rangle^* \langle f | \hat{S} | i \rangle \end{aligned}$$

Expressed in terms of the S-matrix:

$$1 = \sum_f S_{fi}^* S_{fi}$$

Using

$$S_{fi} = \delta_{fi} + i(2\pi)^4 \delta(p_f - p_i) T_{fi}$$

dividing by $i(2\pi)^4 \delta(0)$:

$$\begin{aligned} \frac{1}{i} (T_{ii} - T_{ii}^*) &= \sum_f (2\pi)^4 \delta(p_f - p_i) |T_{fi}|^2 \\ &= 2w \sigma_{\text{tot}} \\ &= 2s \sigma_{\text{tot}} \end{aligned}$$

The l.h.s. :

$$\frac{1}{i} (T_{ii} - T_{ii}^*) = 2\text{Im}T$$

So we get the optical theorem

$$2\text{Im}T_{ii} = \sum_f (2\pi)^4 \delta(p_f - p_i) |T_{fi}|^2 = 2s \sigma_{\text{tot}}$$

Assume:

- T_{ii} is Lorentz invariant \rightarrow use s, t
- $T_{ii}(s, t)$ is an analytic function of s , with s considered as a complex variable
(Hermitean analyticity)
- $T_{ii}(s, t)$ is real on some part of the real axis

Using the Schwarz reflection principle, $T_{ii}(s, t)$ first defined for $\text{Im}s \geq 0$ can be continued in a unique fashion via $T_{ii}(s^*, t) = T_{ii}(s, t)^*$.

So:

$$\frac{1}{i} (T_{ii}(s, t) - T_{ii}(s, t)^*) = \frac{1}{i} (T_{ii}(s, t) - T_{ii}(s^*, t))$$

Def:

$$\text{disc } T = T_{ii}(s + i\epsilon, t) - T_{ii}(s - i\epsilon, t)$$

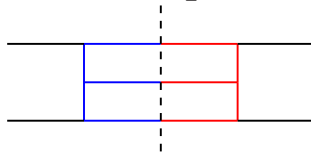
We have finally

$$\frac{1}{i} \text{disc } T = (2\pi)^4 \delta(p_f - p_i) \sum_f |T_{fi}|^2 = 2s \sigma_{\text{tot}}$$

Interpretation: $\frac{1}{i} \text{disc } T$ can be seen as a so-called “cut diagram”, with modified Feynman rules, the “intermediate particles” are on mass shell.

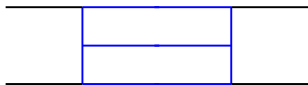
Modified Feynman rules :

- Draw a dashed line from top to bottom



- Use “normal” Feynman rules to the left
- Use the complex conjugate expressions to the right
- For lines crossing the cut: Replace propagators by mass shell conditions $2\pi\theta(p^0)\delta(p^2 - m^2)$

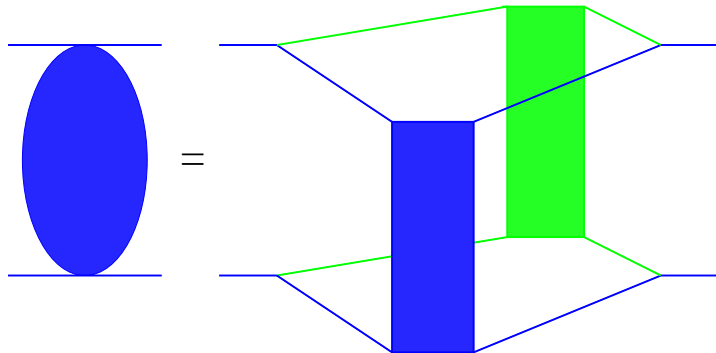
Cutting a diagram representing **elastic** scattering



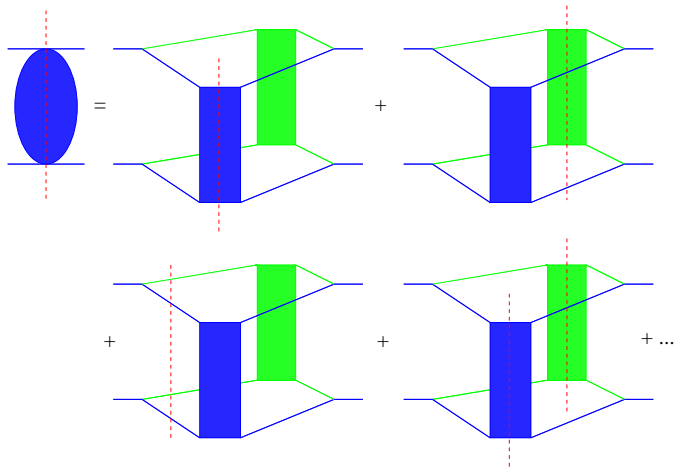
corresponds to **inelastic** scattering

$$\text{Diagram with cut} = \left| \text{Diagram} \right|^2$$

Cutting diagrams is useful in case of substructures:



**Precisely the multiple scattering structure
in EPOS**



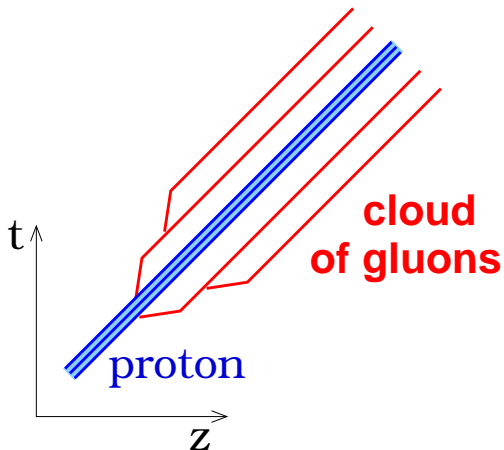
Cut diagram

= sum of products of cut/uncut subdiagrams

=> **Gribov-Regge approach of multiple scattering**

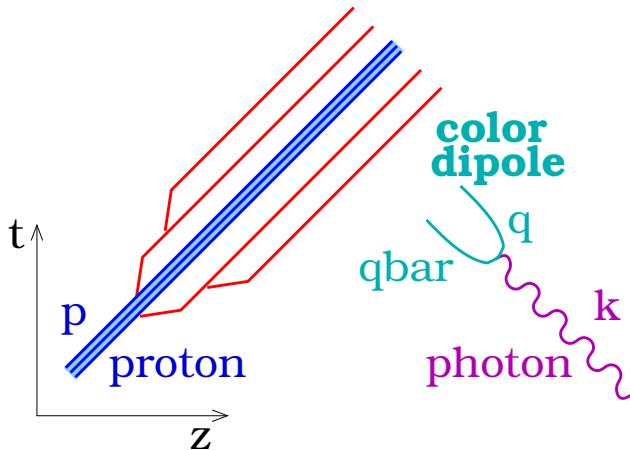
Parton evolution

A fast moving proton



emits successively
partons (mainly
gluons), quasi-
real (large gamma
factors)

... which can be probed by a virtual photon
(emitted from an electron)



photon splits
into q - $qbar$

→ Color dipole

p and k are
proton and
photon mo-
mentum

What precisely the photon “sees” depends on two kinematic variables,

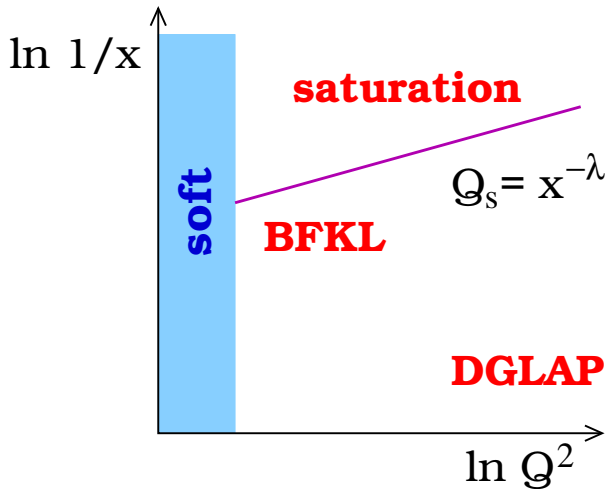
the **virtuality**

$$Q^2 = -k^2$$

and the **Bjorken variable**

$$x = \frac{Q^2}{2pk}$$

which probes partons with momentum fraction x .
It determines also the **approximation scheme** to compute the parton cloud.



DGLAP: summing to all orders of $\alpha_s \ln Q^2$

BFKL: summing to all orders of $\alpha_s \ln \frac{1}{x}$

Linear equations

BFKL (Balitsky, Fadin, Kuraev, and Lipatov):

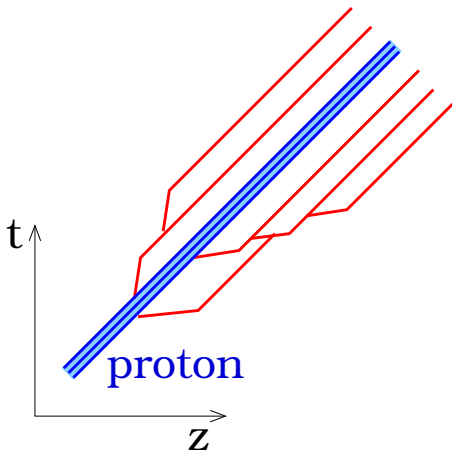
$$\frac{\partial \varphi(x, \mathbf{q})}{\partial \ln \frac{1}{x}} \frac{\alpha_s N_c}{\pi^2} \int d^2 k K(\mathbf{q}, \mathbf{k}) \varphi(x, \mathbf{k})$$

$$\text{with } xg(x, Q^2) = \int_0^{Q^2} \frac{d^2 k}{k^2} \varphi(x, \mathbf{k}),$$

DGLAP (Dokshitzer, Gribov, Lipatov, Altarelli and Parisi):

$$\frac{\partial g(x, Q^2)}{\partial \ln q^2} = \int_x^1 \frac{dz}{z} \frac{\alpha_s}{2\pi} P(z) g\left(\frac{x}{z}, Q^2\right)$$

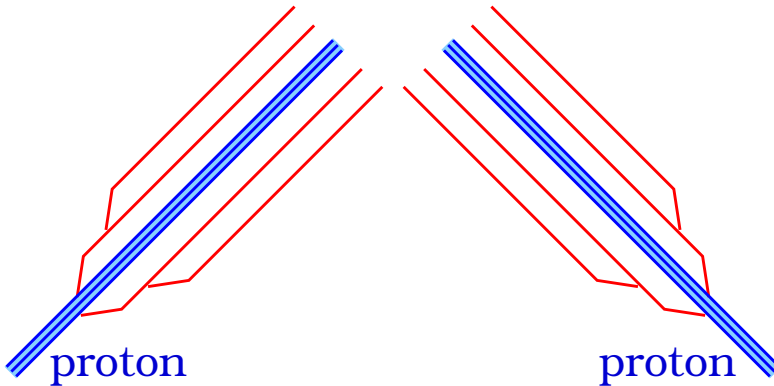
Very large $\ln 1/x$: Saturation domain



Non-linear effects

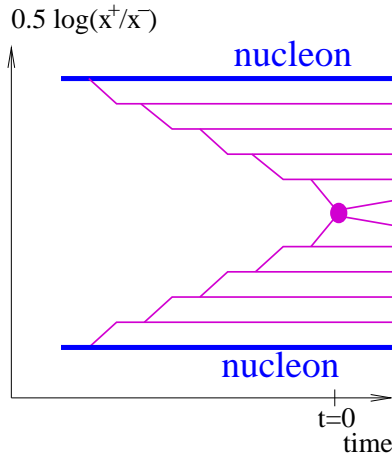
Gluon from one cascade is absorbed by another one

pp scattering (linear domain)



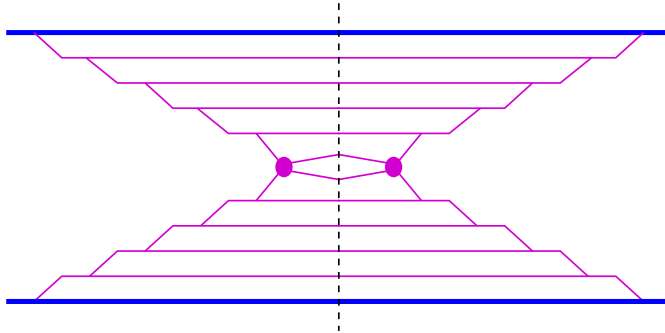
Same evolution as in proton-photon (**causality**)

Different way of plotting the same reaction



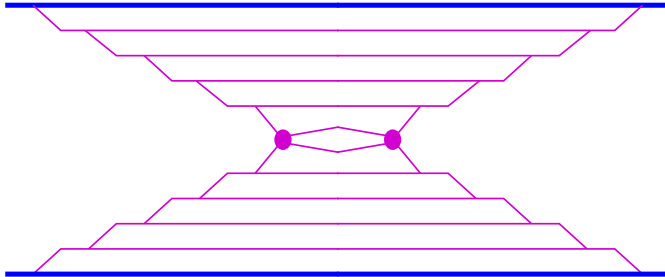
inelastic scattering diagram

Corresponding cut diagram



referred to as **“cut parton ladder”**
= amplitude squared of the inelastic diagram

Corresponding elastic diagram



referred to as **“(uncut) parton ladder”**

Soft domain

Very small $\ln Q^2$: No perturbative treatment!

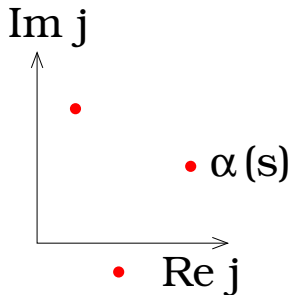
But one may use again the hypothesis of **Lorentz invariance** and **analyticity** of the T-matrix. One starts with a partial wave expansion of the T-matrix (Watson-Sommerfeld transform) :

$$T(t, s) = \sum_{j=0}^{\infty} (2j+1) \mathcal{T}(j, s) P_j(z)$$

with $t \propto z - 1$, $z = \cos \vartheta$, P_j : Legendre polynomials.

With $\alpha(s)$ being the right-most pole of $\mathcal{T}(j, s)$ one gets for $t \rightarrow \infty$:

$$T(t, s) \propto t^{\alpha(s)}$$



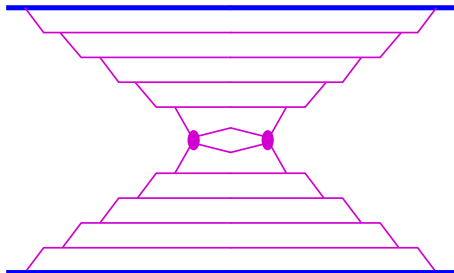
and assuming crossing symmetry one gets the famous asymptotic result

$$T(s, t) \propto s^{\alpha(t)}$$

with the “Regge pole”

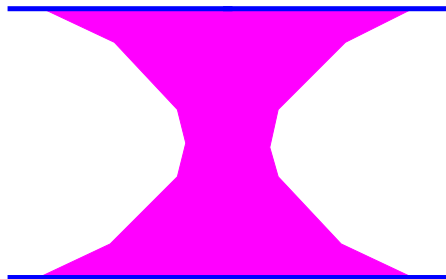
$$\alpha(t) = \alpha(0) + \alpha' t$$

**Perturbative:
Parton ladder**



T-matrix computed
(DGLAP)

**Soft:
Soft Pomeron**



gluons fields

T-matrix parametrized

Formulas (see Phys.Rept. 350 (2001) 93-289):

$$T_{\text{soft}}(\hat{s}, t) = 8\pi s_0 i \gamma_{\text{Pom-parton}}^2 \left(\frac{\hat{s}}{s_0} \right)^{\alpha_{\text{soft}}(0)} \times \exp(\lambda_{\text{soft}} t),$$

with

$$\lambda_{\text{soft}} = 2R_{\text{Pom-parton}}^2 + \alpha'_{\text{soft}} \ln \frac{\hat{s}}{s_0}.$$

Cut soft Pomeron (Schwarz reflection principle):

$$\begin{aligned} & \frac{1}{i} \text{disc } T_{\text{soft}}(\hat{s}, t) \\ &= \frac{1}{i} [T_{\text{soft}}(\hat{s} + i0, t) - T_{\text{soft}}(\hat{s} - i0, t)] \\ &= 2\text{Im } T_{\text{soft}}(\hat{s}, t) \end{aligned}$$

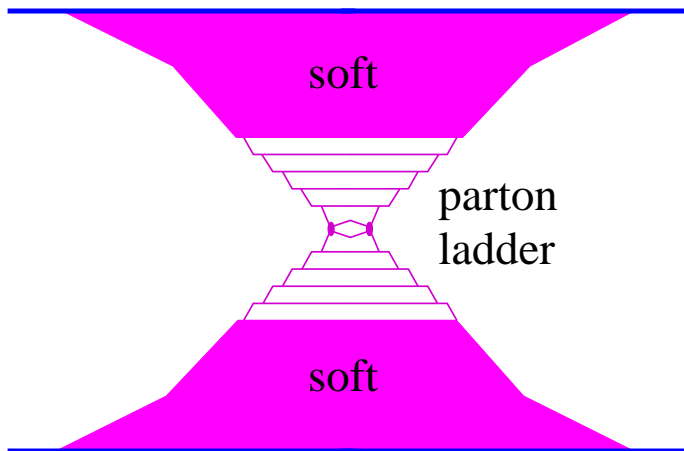
Interaction cross section,

$$\begin{aligned}\sigma_{\text{soft}}(\hat{s}) &= \frac{1}{2\hat{s}} 2\text{Im} T_{\text{soft}}(\hat{s}, 0), \\ &= 8\pi\gamma_{\text{part}}^2 \left(\frac{\hat{s}}{s_0}\right)^{\alpha_{\text{soft}}(0)-1},\end{aligned}$$

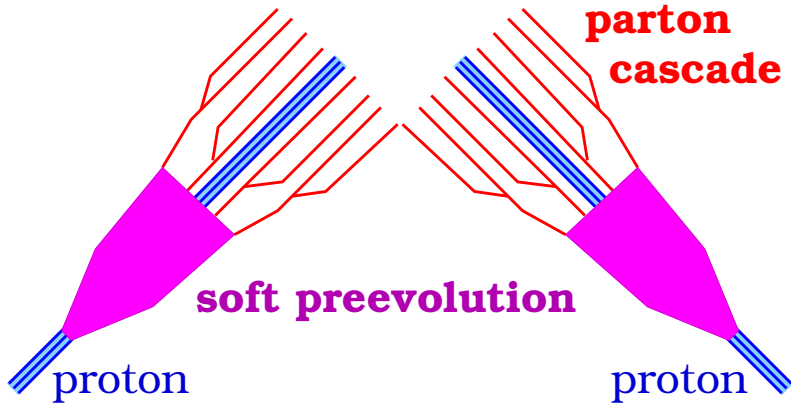
using the optical theorem (with $t = 0$),

which grows faster than data

Semihard Pomeron



Space-time picture of semihard Pomeron



Hard cross section and amplitude (see Phys.Rept. 350 (2001) 93-289) :

$$\begin{aligned} \sigma_{\text{hard}}^{jk}(\hat{s}, Q_0^2) &= \frac{1}{2\hat{s}} 2\text{Im} T_{\text{hard}}^{jk}(\hat{s}, t=0) \\ &= K \sum \int dx_B^+ dx_B^- dp_{\perp}^2 \frac{d\sigma_{\text{Born}}^{ml}}{dp_{\perp}^2}(x_B^+ x_B^- \hat{s}, p_{\perp}^2) \\ &\quad \times E_{\text{QCD}}^{jm\ ml}(x_B^+, Q_0^2, M_F^2) E_{\text{QCD}}^{kl}(x_B^-, Q_0^2, M_F^2) \theta(M_F^2 - Q_0^2), \end{aligned}$$

One knows (Lipatov, 86): amplitude is imaginary, and nearly independent on $t \Rightarrow$ (with $R_{\text{hard}}^2 \simeq 0$) :

$$T_{\text{hard}}^{jk}(\hat{s}, t) = i\hat{s} \sigma_{\text{hard}}^{jk}(\hat{s}, Q_0^2) \exp(R_{\text{hard}}^2 t)$$

Semihard amplitude :

$$iT_{\text{semihard}}(\hat{s}, t) = \sum_{jk} \int_0^1 \frac{dz^+}{z^+} \frac{dz^-}{z^-} \\ \times \text{Im} T_{\text{soft}}^j\left(\frac{s_0}{z^+}, t\right) \text{Im} T_{\text{soft}}^k\left(\frac{s_0}{z^-}, t\right) iT_{\text{hard}}^{jk}(z^+ z^- \hat{s}, t)$$

(valid for $s \rightarrow \infty$ and small parton virtualities except for the ones in the ladder)

Cross sections

(a) Exclusive : $a + b \rightarrow c + d$

(b) Total : $a+b \rightarrow X$ (sum of (a))

(c) Inclusive : $a + b \rightarrow c + X$ (weighted sum of (a))

There are simple formulas for inclusive cross sections (AGK cancellations), but one needs to go beyond when studying high multiplicity pp.

Consider multiple scattering amplitude

$$iT = \prod iT_P$$

cross section: sum over all cuts.

For each cut Pom:

$$\frac{1}{i} \text{disc} T_P = 2 \text{Im} T_P \equiv G$$

For each uncut one:

$$iT_P + \{iT_P\}^* = i(i \text{Im} T_P) + \{i(i \text{Im} T_P)\}^* = -2 \text{Im} T_P \equiv -G$$

Inclusive cross section: weighted sum over all cuts:
The multiplicity for k cut Pomerons is kN , if N is the multiplicity per cut Pomeron.

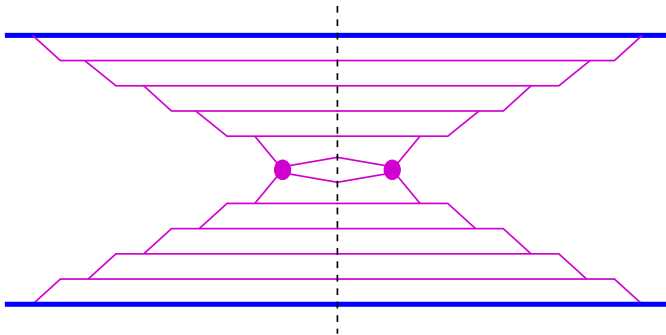
Contribution to the inclusive cross section for n Pomerons:

$$\sigma_{\text{incl}}^{(n)} \propto \sum_{k=0}^n kN G^k (-G)^{n-k} \binom{n}{k} = 0 \text{ for } n > 1$$

Only $n=1$ contributes (single Pomeron) !!

AGK cancellations for $n > 1$

simple diagram even in case of multiple scattering



corresponds to factorization:

$$\sigma_{\text{incl}} = F \otimes \sigma_{\text{elem}} \otimes F$$

Kind of obvious that **factorization** should hold for inclusive cross sections, so

$$\sigma_{\text{incl}} = F \otimes \sigma_{\text{elem}} \otimes F$$

may be used as starting point, with F taken from DIS (photon-proton).

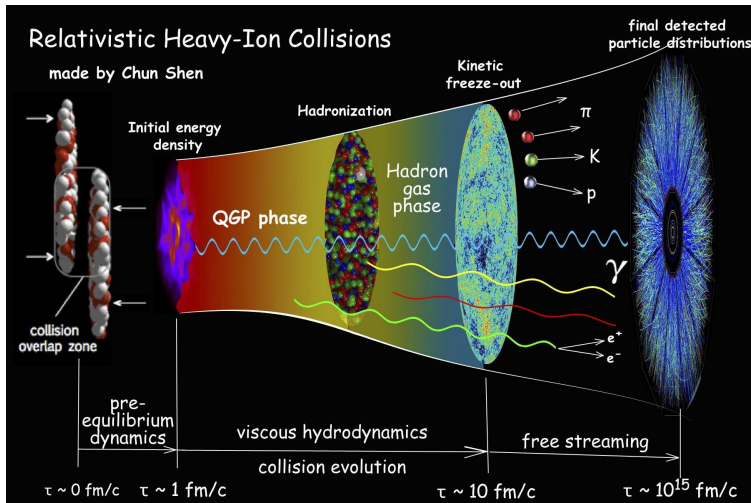
III Model overview

with contributions from T. Pierog, S. Ostapchenko, C. Bierlich,
F. Riehn, P. Tribedy, A. Fedynitch

Models for min bias and high multiplicity pp

model	Gribov Regge	Dipole	Facto risation	used for CR	authors
QGSJETII	X			X	Ostapchenko
EPOSLHC	X			X	Pierog, Werner
EPOS3	X				Werner, Pierog
DIPSY		X			Lönblad, Bierlich
IP-Glasma		X			Tribedy, Schenke
SIBYLL			X	X	Engel, Riehn
DPMJETIII			X	X	Engel, Fedynitch
PYTHIA			X		Sjostrand, Skands
HERWIG			X		Marchesini, Webber

Models for high multipl pp, pA, AA including collective effects



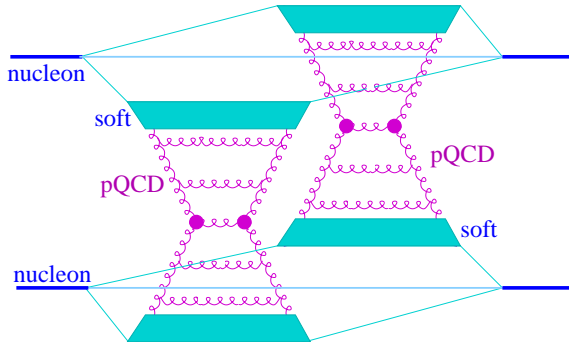
model	primary scatterings	secondary interactions	
EPOS	Gribov Regge	viscous hydrodynamical expansion of QGP	hadronic cascade
IP-Glasma	Dipole model	“	“
Supersonic	Wounded nucleon model	“	“
AMPT	Minijets from Pythia	partonic cascade	“

Cascade means:

Successive scatterings $a + b \rightarrow c + d$ according to known cross sections

Gribov-Regge multiple scattering approach

EPOS, QGSJETII



S-Matrix based
on Pomerons

Pomerons :
Parton ladders (initial
and final state radia-
tion, DGLAP) + soft

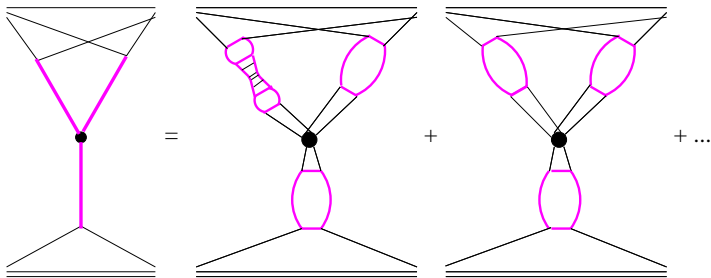
Cutting rules to get
inelastic cross sec-
tions.

Same principle for pp,
pA, AA

more details later

Nonlinear effects in QGSJET

Pomeron-Pomeron coupling



Summing of **all orders**

No energy conservation

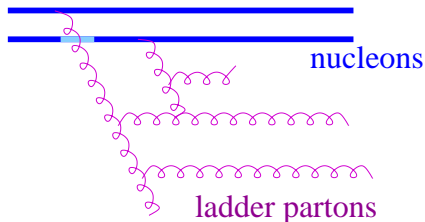
(in EPOS full energy conservation, but effective treatment of nonlinear effects)

Nonlinear effects in EPOS

Nonlinear effects (gluon fusion) taken care of via a saturation scale Q_s

Saturation scale depends on Pomeron energy ($\sqrt{x^+ x^- s}$) and the environment

Selfconsistent procedure within multiple scattering framework (more later)



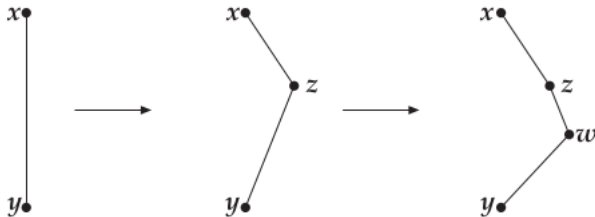
Dipole approach

Initial state radiation in DIPSY (from Christian Bierlich)

Initial nucleon: Three dipoles

LL BFKL in b -space + corrections: A dipole (\vec{x}, \vec{y}) can emit a gluon at position \vec{z} with probability (P) per unit rapidity (Y)

$$\frac{dP}{dY} = \frac{\bar{\alpha}}{2\pi} d^2 \vec{z} \frac{(\vec{x} - \vec{y})^2}{(\vec{x} - \vec{z})^2 (\vec{z} - \vec{y})^2}$$



Multiple scattering

Multiple color exchange

between dipoles i and j
with probabilities

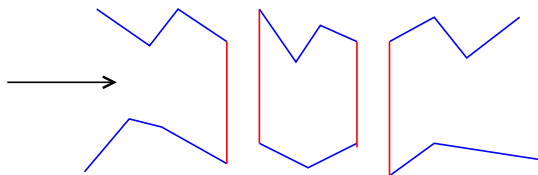
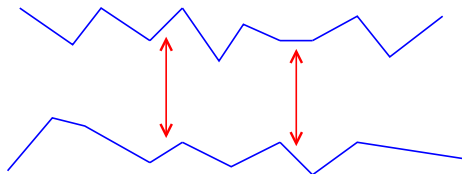
$$\frac{\alpha_s^2}{4} \left[\log \left(\frac{(\vec{x}_i - \vec{y}_j)^2 (\vec{y}_i - \vec{x}_j)^2}{(\vec{x}_i - \vec{x}_j)^2 (\vec{y}_i - \vec{y}_j)^2} \right) \right]^2$$

-> kinky strings

Two “leading” strings

**Additional strings
from loops**

No Remnants



Many strings:
Lund strings may overlap

**=> color ropes
(Larger eff. string tension)**

Initial state in IP-Glasma (from Prithwish Tribedy)

IP-Sat dipole model (r_{\perp} =dipole size):

$$\frac{d\sigma}{d^2b} = 2 [1 - \exp(-F(r_{\perp}, x, b))], \quad F \propto r_{\perp}^2 \alpha_s(\mu^2) xg(x, \mu^2) T(b)$$

$T(b)$: Gaussian profile, $\mu^2 = 4/r_{\perp}^2 + \mu_0^2$, xg : DGLAP evolution

Saturation scale Q_s defined via

$$F\left(r_{\perp}, x = \frac{2}{Q_s^2}, b\right) = \frac{1}{2}$$

IP-Glasma: Color charge squared for projectile A and target B :

$g^2 \mu_A^2 = \sum_{nucleons} g^2 \mu_i^2$, with $g^2 \mu_i^2 \propto Q_s^2$ with Q_s^2 from IP-Sat model.

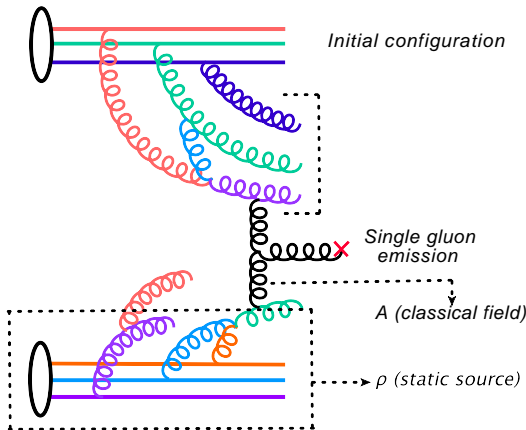
Multiple Scattering

Color charge density $\rho_{A/B}$
 generated from Gaussian
 distribution with variance
 $g^2 \mu_A^2$ (contains DGLAP, satura-
 tion)

Current

$$J^\nu = \delta^{\nu\pm} \rho_{A/B}(x^\mp, x_\perp)$$

Field from $[D_\mu, F_{\mu\nu}] = J_\nu$
 Numerical (lattice) solution,
 fields can be expressed in
 terms of initial ones:
 $A^i = A_A^i + A_B^i, A^\eta = \frac{ig}{2}[A_A^i, A_B^i]$



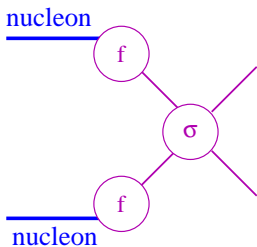
Multiple scattering:

Nonlinearity in terms of A :
 Infinite number of $g + g \rightarrow g$
 processes

Fields \rightarrow Gluons \rightarrow Pythia strings

Models based on factorization

$$\sigma_{\text{jet}} = \int dx_1 dx_2 \int dp_t^2 \sum f_i(x_1, p_t^2) f_j(x_2, p_t^2) \frac{d\sigma_{ij}}{dp_t^2}(\hat{s}, \hat{t}) \quad (A)$$



PYTHIA
HERWIG
SIBYLL
DPMJETIII

First step: σ_{jet} according to (A)

Second step: Multiple scattering scheme via eikonal formula

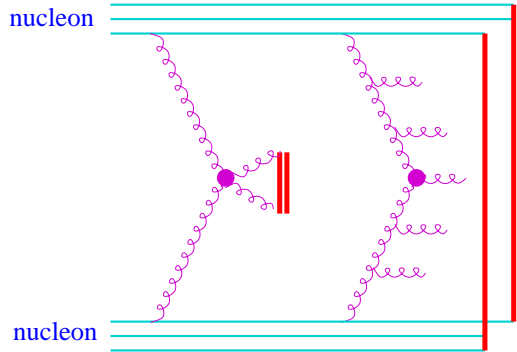
$$\text{prob}(n) = \frac{[\sigma_{\text{jet}}(s) T(s, b)]^n}{n!} \exp(-\sigma_{\text{jet}}(s) T(s, b))$$

Multiple scattering in SIBYLL

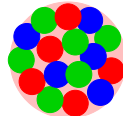
From F. Riehn

Multiple scattering via
eikonal model with soft
and hard component

- No Remnants
- Main scattering
=> qq-q strings
- Further scatterings
=> strings between
gluon pairs



Saturation scale from

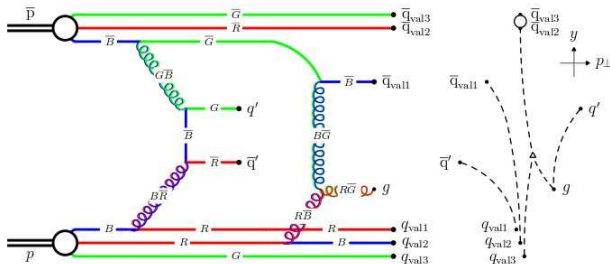
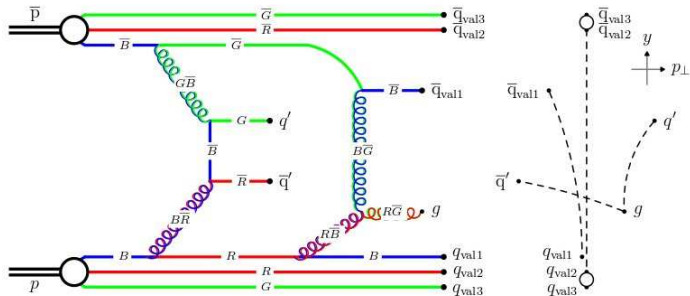


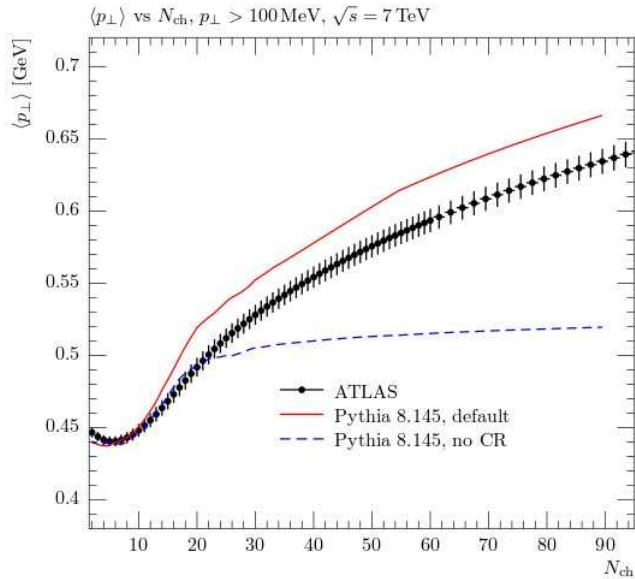
$$\frac{\alpha_s N_c}{Q^2} \times \frac{1}{N_c^2 - 1} \frac{xG}{\pi R^2} = 1$$

Multiple scattering in Pythia

arXiv:1101.2599

Color reconnections



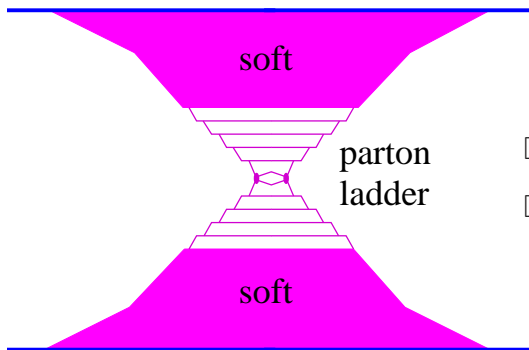


IV Multiple scattering in EPOS

in collaboration with T. Pierog, S. Ostapchenko,
B. Guiot, G. Sophys, , M. Stefaniak

Parton based Gribov-Regge theory. By H.J. Drescher, M. Hladik, S. Ostapchenko, T. Pierog, K. Werner. hep-ph/0007198. Published in Phys.Rept. 350 (2001) 93-289.

Single scattering (single Pomeron)



- Parton emission starts long before the actual interaction (partons are very long-lived due to a large γ).
- **Soft pre-evolution**
- Subsequent parton emissions towards smaller x -values and larger virtualities (from both sides).
- The final partons from either nucleon interact ("hard" collision).

Multiple scattering

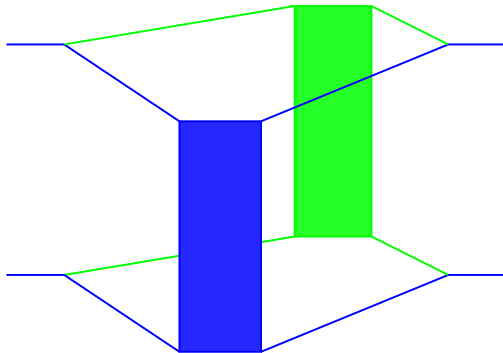
Be T the elastic (pp,pA,AA) scattering T-matrix =>

$$2s \sigma_{\text{tot}} = \frac{1}{i} \text{disc } T$$

Basic assumption : Multiple “Pomerons”

$$iT = \sum_k \frac{1}{k!} \{ iT_{\text{Pom}} \times \dots \times iT_{\text{Pom}} \}$$

Example: 2 “Pomerons”



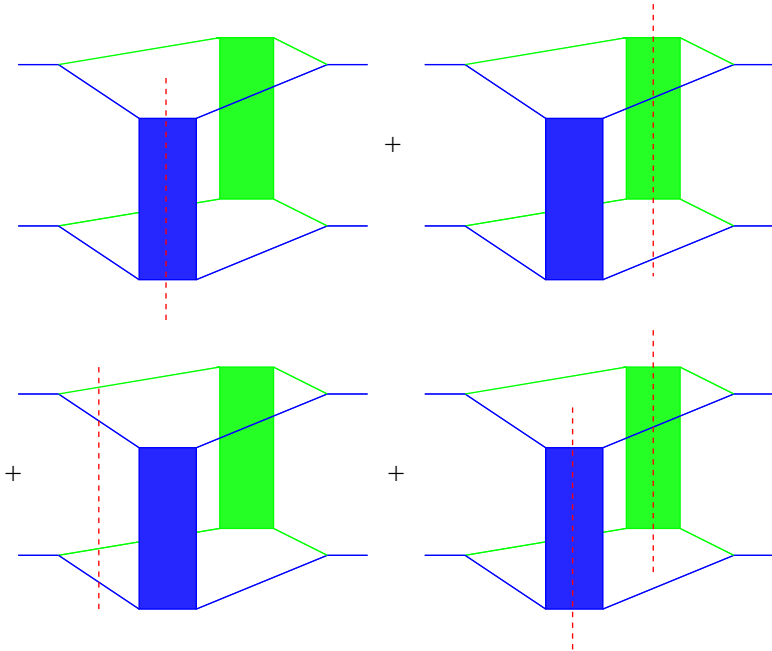
Evaluate

$$\frac{1}{i} \text{disc} \{ iT_{\text{Pom}} \times \dots \times iT_{\text{Pom}} \}$$

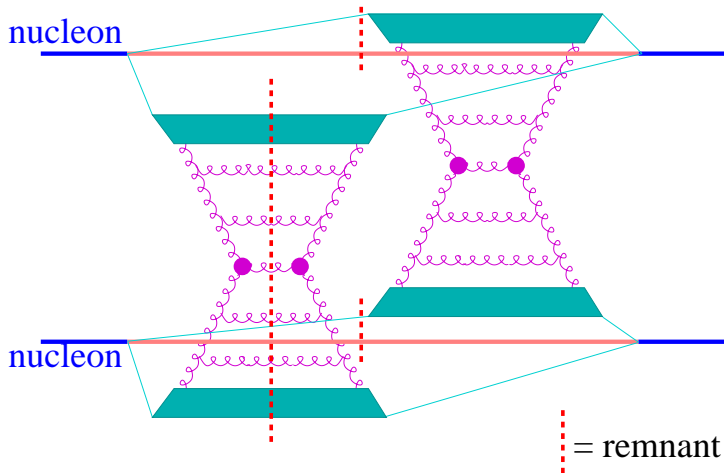
using “cutting rules” :

**A “cut” multi-Pomeron diagram
amounts to the sum of all possible cuts**

Example of two Pomeron



Using “Pomeron = parton ladder + soft”, we have (first diagram)



Using a simplified notation
for “cut” and “uncut” Pomeron



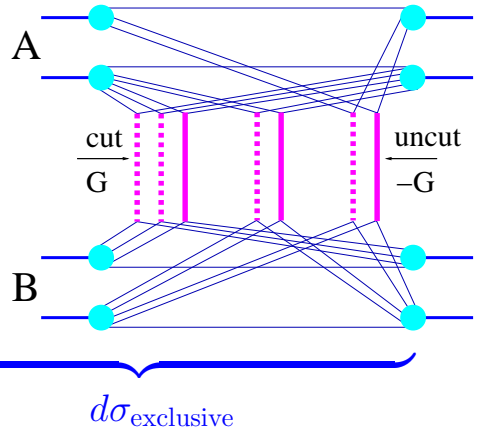
one gets ...

Complete result

(Drescher, Hladik, Ostapchenko, Pierog, and Werner, Phys. Rept. 350, 2001)

For pp, pA, AA:

$$\sigma^{\text{tot}} = \sum_{\text{cut P}} \int \sum_{\text{uncut P}} \int$$



Dotted lines : Cut Pomerons (parton ladders)

$$\begin{aligned}
 \sigma^{\text{tot}} = & \int d^2b \int \prod_{i=1}^A d^2b_i^A dz_i^A \rho_A(\sqrt{(b_i^A)^2 + (z_i^A)^2}) \\
 & \prod_{j=1}^B d^2b_j^B dz_j^B \rho_B(\sqrt{(b_j^B)^2 + (z_j^B)^2}) \\
 & \sum_{m_1 l_1} \dots \sum_{m_{AB} l_{AB}} (1 - \delta_{0 \Sigma m_k}) \int \prod_{k=1}^{AB} \left(\prod_{\mu=1}^{m_k} dx_{k,\mu}^+ dx_{k,\mu}^- \prod_{\lambda=1}^{l_k} d\tilde{x}_{k,\lambda}^+ d\tilde{x}_{k,\lambda}^- \right) \left\{ \right. \\
 & \prod_{k=1}^{AB} \left(\frac{1}{m_k!} \frac{1}{l_k!} \prod_{\mu=1}^{m_k} G(x_{k,\mu}^+, x_{k,\mu}^-, s, |\vec{b} + \vec{b}_{\pi(k)}^A - \vec{b}_{\tau(k)}^B|) \right. \\
 & \left. \left. \prod_{\lambda=1}^{l_k} -G(\tilde{x}_{k,\lambda}^+, \tilde{x}_{k,\lambda}^-, s, |\vec{b} + \vec{b}_{\pi(k)}^A - \vec{b}_{\tau(k)}^B|) \right) \right\} \\
 & \prod_{i=1}^A \left(1 - \sum_{\pi(k)=i} x_{k,\mu}^+ - \sum_{\pi(k)=i} \tilde{x}_{k,\lambda}^+ \right)^\alpha \prod_{j=1}^B \left(1 - \sum_{\tau(k)=j} x_{k,\mu}^- - \sum_{\tau(k)=j} \tilde{x}_{k,\lambda}^- \right)^\alpha \left. \right\}
 \end{aligned}$$

□ **Complicated with energy sharing included**

(10,000,000-dimensional integrals)

□ **but doable**

- **Parameterizations for $G(x^+, x^-, s, b)$**
- **Analytical integrations**
- **Employing Markov chain techniques**

Step 1:

- We compute **partial cross sections** σ_K for particular configurations K via analytical integration
- K is a multi-dimensional variable
for example for double scattering in pp with two Pomerons involved: $K = \{x_1^+, x_1^-, \vec{p}_{t1}, x_2^+, x_2^-, \vec{p}_{t2}\}$
- Configurations K in AA scattering may be quite complex

Step 2:

The partial cross sections σ_K can be

- interpreted as **probability distributions**,
- enabling us to use Monte Carlo techniques to **generate configurations** K .

Since we are dealing with multidimensional probability distributions, we have to employ very sophisticated

Markov chain techniques

to generate configurations according to Ω .

Configurations via Markov chains
(the heart of EPOS, see Phys. Rept. 350, 2001)

Consider a sequence of multidimensional random numbers

$$x_1, x_2, x_3, \dots$$

with f_t being the law for x_t .

A homogeneous Markov chain is defined as

$$f_t(x) = \sum_{x'} f_{t-1}(x') p(x' \rightarrow x).$$

with $p(x' \rightarrow x)$ being the transition probability (or matrix). Normalization : $\sum_x p(x' \rightarrow x) = 1$.

Let f be the law for x_t . The law for x_{t+1} is

$$\sum_a f(a) p(a \rightarrow b).$$

One defines an operator T (comme Translation)

$$Tf(b) = \sum_a f(a) p(a \rightarrow b).$$

So Tf is the law for x_{t+1} when f is the law for x_t .

A law is called stationary if $Tf = f$.

Theorem: If a stationary law $Tf = f$ exists, then $T^k f_1$ converges towards f (which is unique) for any f_1 .

So to generate (multidimensional) random numbers according to some (given) law f ,

- one constructs a T such that $Tf = f$
- and then iterates $T^k f_1$

One needs, for a given law f ,
to **find a transition matrix p such that $Tf = f$**

Sufficient condition (detailed balance):

$$f(a) p(a \rightarrow b) = f(b) p(b \rightarrow a),$$

Proof :

$$\begin{aligned} Tf(b) &= \sum_a f(a) p(a \rightarrow b) \\ &= \sum_a f(b) p(b \rightarrow a) \\ &= f(b) \sum_a p(b \rightarrow a) \\ &= f(b). \end{aligned}$$

Metropolis algorithm

Definitions:

$$p_{ab} = p(a \rightarrow b),$$
$$f_a = f(a).$$

Take

$$p_{ab} = w_{ab} u_{ab}. \quad (a \neq b).$$

with

w_{ab} : proposal matrix ($\sum_b w_{ab} = 1$)

u_{ab} : acceptance matrix ($u_{ab} \leq 1$)

This is NOT the simple acceptance-rejection method!!

Detailed balance:

$$f_a p_{ab} = f_b p_{ba}$$

amounts to

$$f_a w_{ab} u_{ab} = f_b w_{ba} u_{ba} ,$$

or

$$\frac{u_{ab}}{u_{ba}} = \frac{f_b w_{ba}}{f_a w_{ab}} .$$

$$\frac{u_{ab}}{u_{ba}} = \frac{f_b}{f_a} \frac{w_{ba}}{w_{ab}}.$$

is solved by

$$u_{ab} = F \left(\frac{f_b}{f_a} \frac{w_{ba}}{w_{ab}} \right),$$

with a function F with

$$\frac{F(z)}{F\left(\frac{1}{z}\right)} = z.$$

Proof : With $z \equiv \frac{f_b}{f_a} \frac{w_{ba}}{w_{ab}}$ one finds : $\frac{u_{ab}}{u_{ba}} = \frac{F(z)}{F\left(\frac{1}{z}\right)} = z = \frac{f_b}{f_a} \frac{w_{ba}}{w_{ab}}.$

The F according to Metropolis is

$$F(z) = \min(z, 1).$$

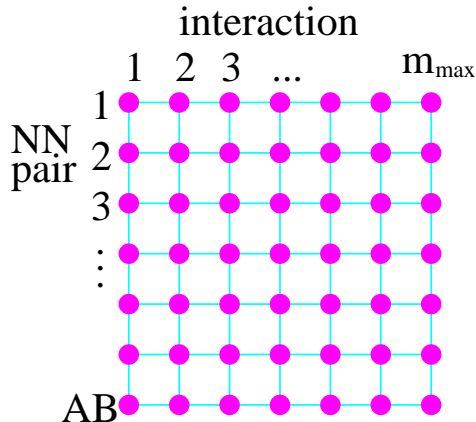
One finds indeed

$$\frac{F(z)}{F(\frac{1}{z})} = \frac{\min(z, 1)}{\min(\frac{1}{z}, 1)} = \begin{cases} z/1 & \text{pour } z \leq 1 \\ 1/\frac{1}{z} & \text{pour } z > 1 \end{cases} = z.$$

So one proposes for each iteration a new configuration b according to some w_{ab} , and accepts it with probability

$$u_{ab} = \min \left(\frac{f_b}{f_a} \frac{w_{ba}}{w_{ab}}, 1 \right).$$

Configuration lattice, define w_{ab} such that b changes w.r.t. a only on one lattice site (like Ising model Metropolis)



Long iterations, but allows to generate very complex configurations according to very complex laws.

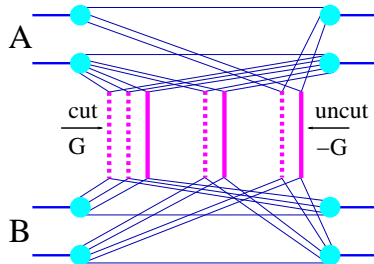
Particle production

Generating “configurations” is only half the story:

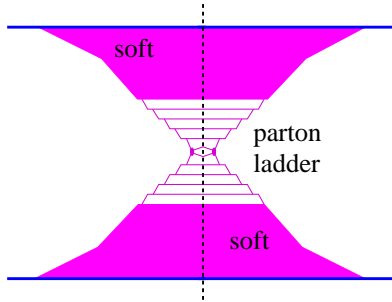
How do we obtain the corresponding partons which “make” the ladder, and finally the hadrons?

(for a given ladder, given momenta and flavors at the endpoints)

For particle production, only the cut Pomeron plays a role



the uncut ones have been summed over



Reminder: in order to compute the contribution of a cut Pomeron to a partial cross section, we sum over emitted partons, integrate over all momenta.

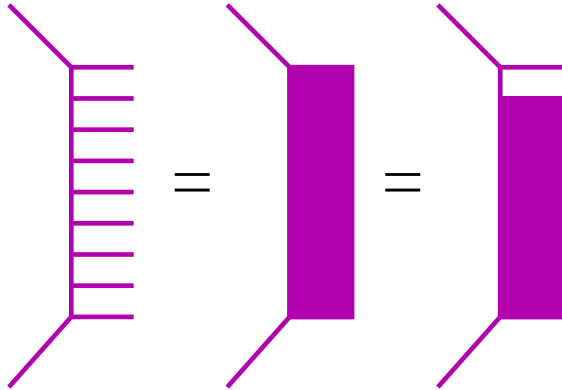
Consistency requires to use these same formulas to obtain probability distributions for the parton emissions (what we do).

Realization: big tables with pre-calculated cross sections, to be used via interpolation to generate partons according to iterative equations.

$$\begin{aligned} \sigma_{\text{hard}}^{ij}(\hat{s}, Q_1^2, Q_2^2) &= \sum_k \int \frac{dQ^2}{Q^2} \int d\xi \Delta^i(Q_1^2, Q^2) \frac{\alpha_s}{2\pi} P_i^k(\xi) \sigma_{\text{hard}}^{kj}(\xi \hat{s}, Q^2, Q_2^2) \\ &+ \sigma_{\text{ord}}^{ji}(\hat{s}, Q_2^2, Q_1^2) \end{aligned}$$

$$\begin{aligned} \sigma_{\text{ord}}^{ij}(\hat{s}, Q_1^2, Q_2^2) &= \sum_k \int \frac{dQ^2}{Q^2} \int d\xi \Delta^i(Q_1^2, Q^2) \frac{\alpha_s}{2\pi} P_i^k(\xi) \sigma_{\text{ord}}^{kj}(\xi \hat{s}, Q^2, Q_2^2) \\ &+ \sigma_{\text{Born}}^{ij}(\hat{s}, Q_1^2, Q_2^2) \end{aligned}$$

$$\begin{aligned} \sigma_{\text{Born}}^{ij}(\hat{s}, Q_1^2, Q_2^2) &= K \int dp_{\perp}^2 \frac{d\sigma_{\text{Born}}^{ij}}{dp_{\perp}^2}(\hat{s}, p_{\perp}^2) \\ &\times \Delta^i(Q_1^2, M_{\text{F}}^2) \Delta^j(Q_2^2, M_{\text{F}}^2) \Theta(M_{\text{F}}^2 - \max[Q_1^2, Q_2^2]) \end{aligned}$$



Probability of single emission:

$$prob(\xi, Q^2) = \frac{dQ^2}{Q^2} \Delta^i(Q_1^2, Q^2) \frac{\alpha_s}{2\pi} P_i^k(\xi) \sigma_{\text{hard}}^{kj}(\xi \hat{s}, Q^2, Q_2^2)$$

From partons to strings:

For $t > 0$, a (cut) Pomeron represents actually a (mainly) **longitudinal color field**,

where the ladder rungs (gluons) represent small transverse momentum components⁽¹⁾.



longitudinal
electric
field

= color string

⁽¹⁾ Lund model idea, first e^+e^- ,
then generalized to pp , see also CGC

Realization:

One-dimensional character of the fields

=> classical string theory

(which does not use much more than some general symmetries)

□ **Mapping: parton ladders -> kinky strings**
(parton momentum = kink)

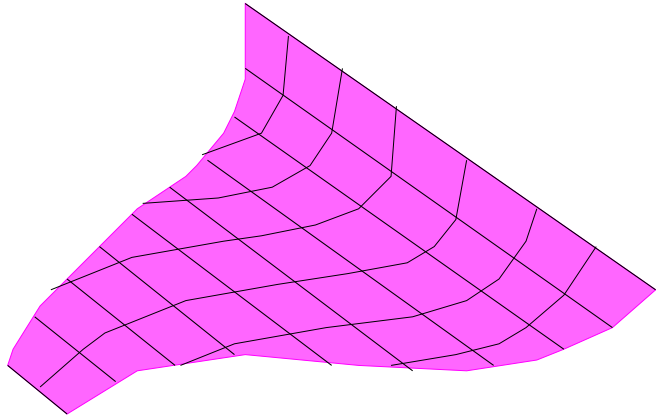
□ **Classical string evolution + decay via area law**

String:

two-
dimensional
surface

$$x(\sigma, \tau)$$

in
Minkowski
space



Break probability :

$$dP = p_B dA,$$

In detail: The string surface is given as

$$x^\mu(\sigma, \tau) = x_0 + \frac{1}{2} \int_{\sigma-\tau}^{\sigma+\tau} g^\mu(\xi) d\xi,$$

so it is completely given in terms of some function $g^\mu(\xi)$ with

$$g^\mu(\sigma) = \dot{x}^\mu(\sigma, \tau = 0).$$

We consider only strings with a piecewise constant initial velocity g , which are called kinky strings.

- **This string is characterized by a sequence of σ intervals $[\sigma_k, \sigma_{k+1}]$, and the corresponding constant values (say v_k) of g in these intervals.**

Such an interval with the corresponding constant value of g is referred to as “kink”.

A parton ladder represents a **sequence of partons** of the type $q - g \dots - g - \bar{q}$, with soft “end partons” q and \bar{q} , and hard inner gluons g .

The mapping “partons \rightarrow string” is done such that we **identify a parton sequence with a kinky string**

by requiring “parton = kink”,

with $\sigma_{k+1} - \sigma_k = \text{energy of parton } k$

and $v_k = \text{momentum of parton } k / E_k$.

What is really done (PR 232, pp 87-299, 1993, PR 350, pp 93-289, 2001):

A string represents a two-dimensional surface in Minkowski space

$$x = x(\sigma, \tau),$$

with σ being a space-like and τ a time-like parameter.

In order to obtain the equations of motion, we need a Lagrangian. It is obtained by demanding the invariance of the action with respect to gauge transformations. This way one finds the Lagrangian of Nambu-Goto:

$$L = -\kappa \sqrt{(x' \dot{x})^2 - x'^2 \dot{x}^2},$$

with “dot” and “prime” referring to the partial derivatives with respect to σ and τ , and with κ being the string tension.

With this Lagrangian we get the Euler-Lagrange equations of motion:

$$\frac{\partial}{\partial \tau} \frac{\partial L}{\partial \dot{x}_\mu} + \frac{\partial}{\partial \sigma} \frac{\partial L}{\partial x'_\mu} = 0.$$

We use the gauge fixing

$$x'^2 + \dot{x}^2 = 0 \text{ and } x' \dot{x} = 0,$$

which provides a very simple equation of motion, namely a wave equation,

$$\frac{\partial^2 x_\mu}{\partial \tau^2} - \frac{\partial^2 x_\mu}{\partial \sigma^2} = 0,$$

with the boundary conditions:

$$\partial x_\mu / \partial \sigma = 0, \quad \sigma = 0, \pi.$$

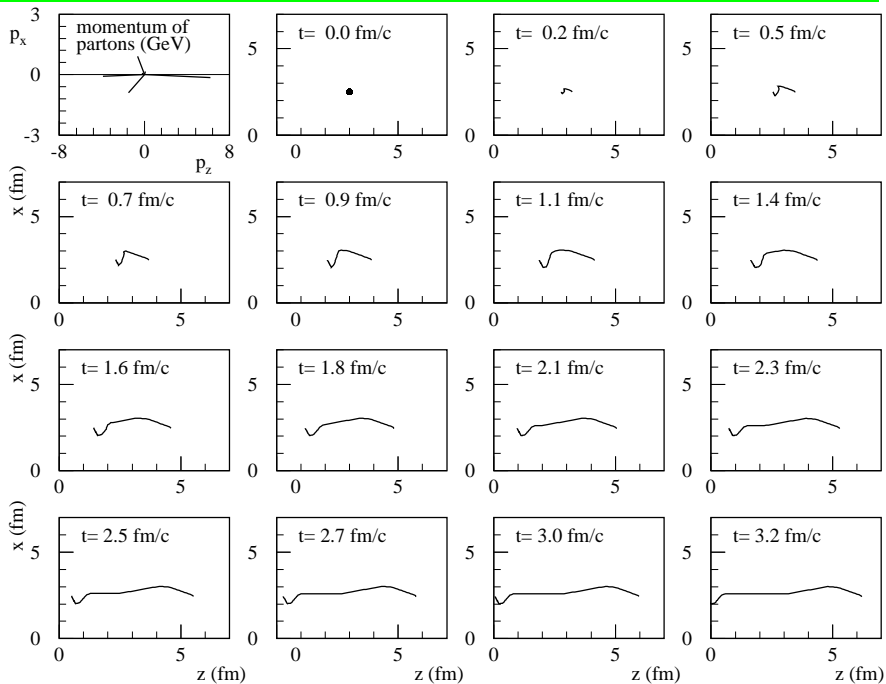
The solution of the equation of motion (with initial extension zero) is

$$x^\mu(\sigma, \tau) = x_0 + \frac{1}{2} \left(\int_{\sigma-\tau}^{\sigma+\tau} g^\mu(\xi) d\xi \right),$$

where g is the initial velocity, $g(\sigma) = \dot{x}(\sigma, \tau)_{\tau=0}$.

Strings are classified according to the function g . Strings with piecewise constant g are called kinky strings, each segment being called kink, finally identified with perturbative partons.

In the following figure, we show the evolution of a string generated in electron-positron annihilation (4 internal kinks).



Hadron production

is finally realized via string breaking, such that string fragments are identified with hadrons.

Hypothesis: the string breaks within an infinitesimal area dA on its surface with a probability which is proportional to this area,

$$dP = p_B dA,$$

where p_B is the fundamental parameter of the procedure. ¹

¹Elegant realization, making use of the dynamics of strings with piecewise constant initial conditions.

A string break is realized via **quark-antiquark** or **diquark-antidiquark** pair production with probability

$$p_{i(j)} = \frac{1}{Z} \exp \left(-\pi \frac{M_{i(j)}^2}{\kappa} \right)$$

with

$$M_{ij} = M_i + M_j + c_i c_j M_0$$

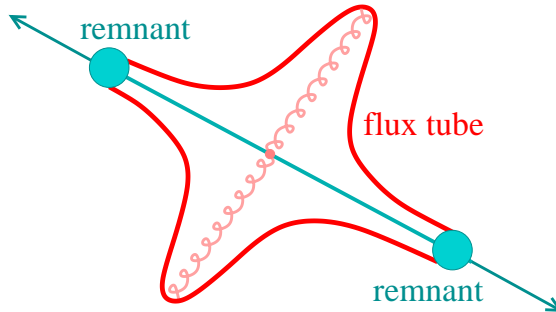
Transverse momenta \vec{p}_t and $-\vec{p}_t$ are generated at each breaking, according to

$$f(k) \propto e^{-|\vec{p}_t|/2\bar{p}_t}, \quad (1)$$

with a parameter \bar{p}_t .

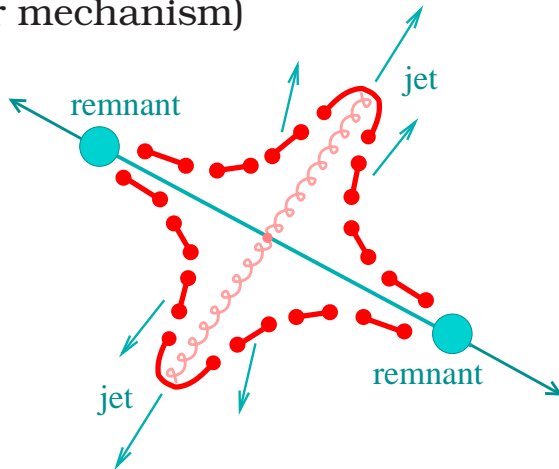
Jets:

Parton ladder = color flux tubes = **kinky strings**



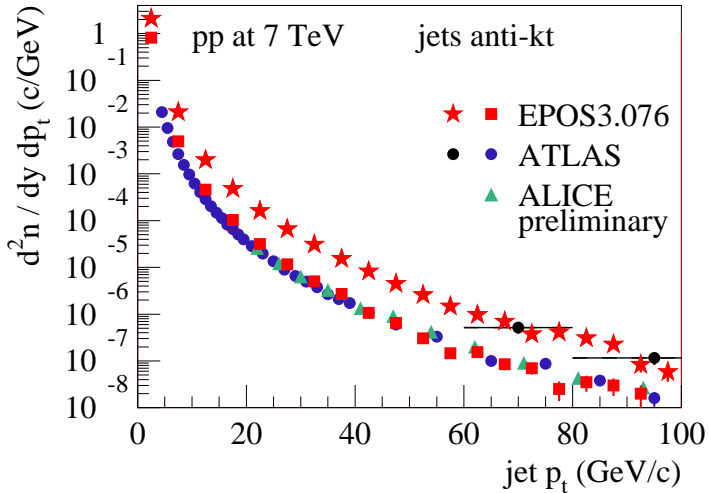
(here no IS radiation, only hard process producing two gluons)

which expand and break
via the production of quark-antiquark pairs
(Schwinger mechanism)

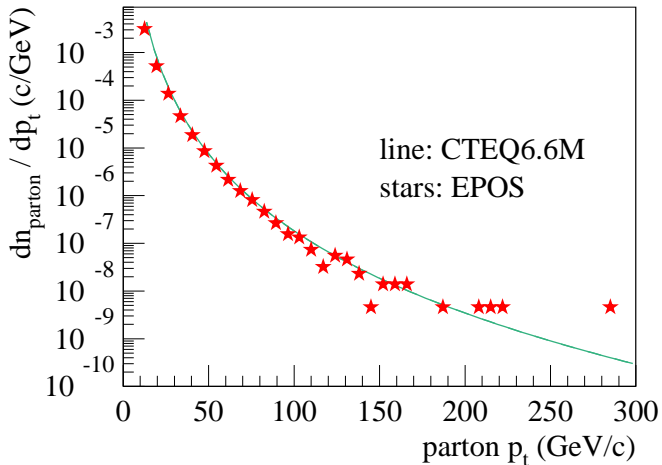


String segment = hadron. Close to "kink": jets

Check: jet production in pp at 7 TeV



Comparison with parton model calculation using CTEQ PDFs for pp at 7 TeV



V Collectivity in EPOS

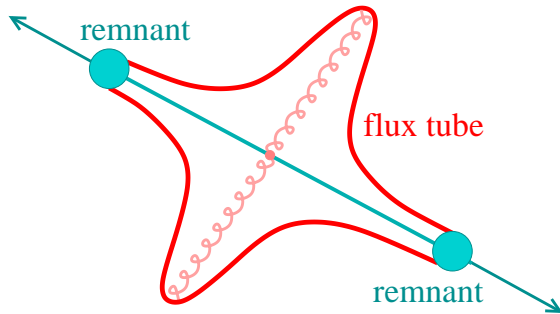
Heavy ion collisions or high energy & high multiplicity pp events:

- the usual procedure has to be modified, since the density of strings will be so high that they cannot possibly decay independently

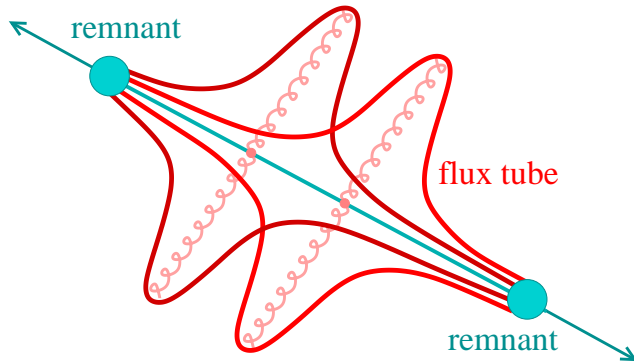
**Some string pieces will constitute bulk matter,
others show up as jets**

These are the same strings (all originating from hard processes at LHC) which constitute BOTH jets and bulk !!

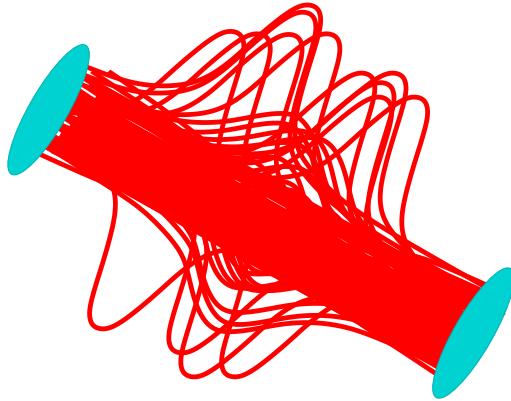
again: single scattering => 2 color flux tubes



... two scatterings => 4 color flux tubes



... many scatterings (AA) => many color flux tubes

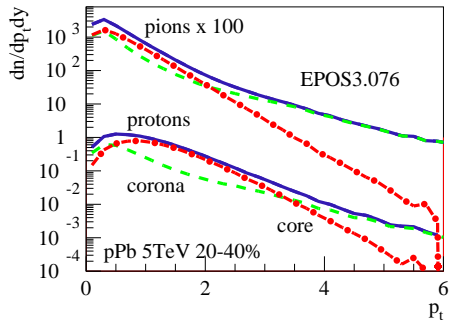
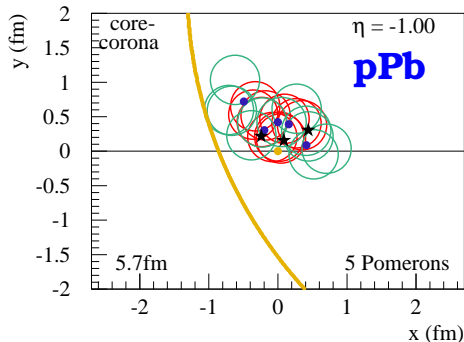


=> matter + escaping pieces (jets)

Core-corona procedure (for pp, pA, AA):

Pomeron => parton ladder => flux tube (kinky string)

String segments with high p_t escape => **corona**,
 the others form the **core** = initial condition for hydro
 depending on the local string density

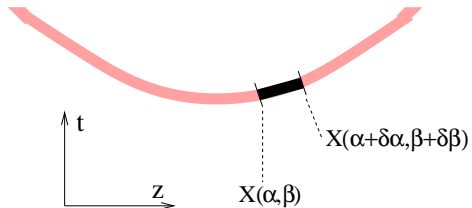


Core:

(we use α and β rather than σ and τ)

We split each string into a sequence of string segments, corresponding to widths $\delta\alpha$ and $\delta\beta$ in the string parameter space

Picture is schematic:
the string extends well into the transverse dimension, correctly taken into account in the calculations



Energy momentum tensor and the flavor flow vector at some position x at initial proper time $\tau = \tau_0$:

$$T^{\mu\nu}(x) = \sum_i \frac{\delta p_i^\mu \delta p_i^\nu}{\delta p_i^0} g(x - x_i),$$

$$N_q^\mu(x) = \sum_i \frac{\delta p_i^\mu}{\delta p_i^0} q_i g(x - x_i),$$

$q \in u, d, s$: net flavor content of the string segments

$\delta p = \left\{ \frac{\partial X(\alpha, \beta)}{\partial \beta} \delta \alpha + \frac{\partial X(\alpha, \beta)}{\partial \alpha} \delta \beta \right\}$: four-momenta of the segments.

g : Gaussian smoothing kernel with a transverse width σ_\perp

The Lorentz transformation into the comoving frame provides the energy density ε and the flow velocity components v^i .

The evolution of the system for $\tau \geq \tau_0$ treated **macroscopically**, solving the equations of **relativistic hydrodynamics**:

Three equations concerning conserved currents:

$$\partial_\nu N_q^\nu = 0$$

with

$$N_q^\nu = n_q u^\nu$$

and n_q ($q = u, d, s$) representing (net) quark densities, u^ν is the velocity four vector.

Four equations concerning energy-momentum conservation:

$$\partial_\nu T^{\mu\nu} = 0.$$

The energy-momentum tensor $T^{\mu\nu}$ is

- the flux of the μ th component of the momentum vector
- across a surface with constant ν coordinate (using four-vectors)

T^{00} : **Energy density** $dE/dx^1 dx^2 dx^3$ (x^0 const)

T^{01} : **Energy flux** $dE/dx^0 dx^2 dx^3$ (x^1 const)

T^{i0} : **Momentum density**

T^{ij} : **Momentum flux**

The equation

$$\partial_\nu T^{\mu\nu} = 0$$

is very general, no need for thermal equilibrium, no need for particles.

The energy-momentum tensor is

the **conserved Noether current**

associated with **space-time translations**.

- We have $4 + n_f$ equations, so we should express T in terms of 4 quantities (unknowns)
- and/or find additional equations
- which means additional assumptions

First approach: **Ideal Fluid**

In the local rest frame of a fluid cell:

- $T^{00} = \varepsilon$ (energy density in LRF)
- $T^{0i} = 0$ (no energy flow)
- $T^{0i} = 0$ (no momentum in LRF)
- $T^{ij} = \delta_{ij}p$ (p = isotropic pressure)

In arbitrary frame:

$$T^{\mu\nu} = (\varepsilon + p)u^\mu u^\nu - pg^{\mu\nu}$$

+ Equation of state $p = p(\varepsilon)$ of QGP from IQCD

=> 4 equations for 4 unknowns (ε , velocity)

Other way of writing T :

$$T^{\mu\nu} = \varepsilon u^\mu u^\nu - p \Delta^{\mu\nu}$$

with Δ being the projector \perp to u ($\Delta^{\mu\nu} u_\nu = 0$):

$$\Delta^{\mu\nu} = g^{\mu\nu} - u^\mu u^\nu$$

Including viscous effects, following Landau:

Navier Stokes equations (with shear and bulk viscosity η, ζ):

$$T^{\mu\nu} = \varepsilon u^\mu u^\nu - (p + \Pi) \Delta^{\mu\nu} + \pi^{\mu\nu}$$

$$\pi^{\mu\nu} = \pi_{NS}^{\mu\nu} = 2\eta \nabla^{\langle\mu} u^{\nu\rangle},$$

$$\Pi = \Pi_{NS} = -\zeta \nabla_\alpha u^\alpha$$

$$A_{\langle\mu} B_{\nu\rangle} = \frac{1}{2} (\Delta_\mu^\alpha \Delta_\nu^\beta + \Delta_\nu^\alpha \Delta_\mu^\beta - \frac{2}{3} \Delta^{\alpha\beta} \Delta_{\mu\nu}) A_\alpha B_\beta, \quad \nabla^\mu = \Delta^{\mu\nu} \partial_\nu$$

$\pi^{\mu\nu}$, Π shear stress tensor, bulk pressure

NS does not work:

- instabilities due to acausal behavior

Solution (Israel-Steward):

$$T^{\mu\nu} = \varepsilon u^\mu u^\nu - (p + \Pi) \Delta^{\mu\nu} + \pi^{\mu\nu}$$

$$\pi^{\mu\nu} = \pi_{\text{NS}}^{\mu\nu} + \tau_\pi (-D\pi^{\mu\nu} + I_\pi^{\mu\nu}),$$

$$\Pi = \Pi_{\text{NS}} + \tau_\Pi (-D\Pi + I_\Pi)$$

$$\text{with } D = u^\mu \partial_\mu$$

Different choices for the I . Implemented in EPOS3 by Y. Karpenko:

$$I_\pi^{\mu\nu} = -\frac{4}{3}\pi^{\mu\nu}\partial_\gamma u^\gamma - [u^\nu\pi^{\mu\beta} + u^\mu\pi^{\nu\beta}]u^\lambda\partial_\lambda u_\beta, \quad I_\Pi = -\frac{4}{3}\Pi\partial_\gamma u^\gamma$$

EPOS implementation (Yuri Karpenko)

Milne coordinates:

$$\begin{aligned}\eta &= \frac{1}{2} \ln \frac{t+z}{t-z} \\ \tau &= \sqrt{t^2 - z^2}\end{aligned}$$

Metric tensor:

$$g^{\mu\nu} = \text{diag}(1, -1, -1, -1/\tau^2).$$

Nonzero Christoffel symbols:

$$\Gamma_{\tau\eta}^{\eta} = \Gamma_{\eta\tau}^{\eta} = 1/\tau, \quad \Gamma_{\eta\eta}^{\tau} = \tau.$$

The hydrodynamic equations (using covariant derivatives):

$$\partial_{;\nu} T^{\mu\nu} = \partial_{\nu} T^{\mu\nu} + \Gamma_{\nu\lambda}^{\mu} T^{\nu\lambda} + \Gamma_{\nu\lambda}^{\nu} T^{\mu\lambda} = 0$$

Freeze out

happens at a hypersurface defined by $T = T_H$ (for given T_H).

Hyper-surface: $x^\mu = x^\mu(\tau, \varphi, \eta)$:

$$x^0 = \tau \cosh \eta, \quad x^1 = r \cos \varphi, \quad x^2 = r \sin \varphi, \quad x^3 = \tau \sinh \eta,$$

with $r = r(\tau, \varphi, \eta)$.

The hypersurface element is

$$d\Sigma_\mu = \varepsilon_{\mu\nu\kappa\lambda} \frac{\partial x^\nu}{\partial \tau} \frac{\partial x^\kappa}{\partial \varphi} \frac{\partial x^\lambda}{\partial \eta} d\tau d\varphi d\eta,$$

(with $\varepsilon^{0123} = 1$)

Computing the derivatives, one gets:

$$d\Sigma_0 = \left\{ -r \frac{\partial r}{\partial \tau} \tau \cosh \eta + r \frac{\partial r}{\partial \eta} \sinh \eta \right\} d\tau d\varphi d\eta,$$

$$d\Sigma_1 = \left\{ \frac{\partial r}{\partial \varphi} \tau \sin \varphi + r \tau \cos \varphi \right\} d\tau d\varphi d\eta,$$

$$d\Sigma_2 = \left\{ -\frac{\partial r}{\partial \varphi} \tau \cos \varphi + r \tau \sin \varphi \right\} d\tau d\varphi d\eta,$$

$$d\Sigma_3 = \left\{ r \frac{\partial r}{\partial \tau} \tau \sinh \eta - r \frac{\partial r}{\partial \eta} \cosh \eta \right\} d\tau d\varphi d\eta.$$

Cooper-Frye hadronization amounts to calculating

$$E \frac{dn}{d^3p} = \int d\Sigma_\mu p^\mu f(up),$$

with u being the flow four-velocity in the global frame, related to Milne fram via

$$\begin{aligned} u^0 &= \tilde{u}^0 \cosh \eta + \tilde{u}^3 \sinh \eta, \\ u^1 &= \tilde{u}^1, \\ u^2 &= \tilde{u}^2, \\ u^3 &= \tilde{u}^0 \sinh \eta + \tilde{u}^3 \cosh \eta. \end{aligned}$$

Similarly p expressed in terms of \tilde{p} in the Milne frame.

f is the Bose-Einstein or Fermi-Dirac distribution.

Hadronic afterburner: UrQMD

After “hadronization” hadrons follow straight and may still interact via

$$h_1 + h_2 \rightarrow \sum_j h'_j$$

We use “UrQMD”.

M. Bleicher et al., J. Phys. G25 (1999) 1859;

H. Petersen, J. Steinheimer, G. Burau, M. Bleicher and H. Stoecker, Phys. Rev. C78 (2008) 044901

VI Flow in small systems

=> comparing models

with / without collectivity built in

pPb results (more results: arXiv:1312.1233)

We will compare EPOS3 with data

and also with

EPOS LHC

LHC tune of EPOS1.99, :

same GR, but uses **parameterized flow**

T. Pierog et al, arXiv:1306.5413

AMPT

Parton + hadron cascade -> **some collectivity**

Z.-W. Lin, C. M. Ko, B.-A. Li, B. Zhang and S. Pal, Phys. Rev. C 72, 064901 (2005).

QGSJET

GR approach, **no flow**

S. Ostapchenko, Phys. Rev. D74 (2006) 014026

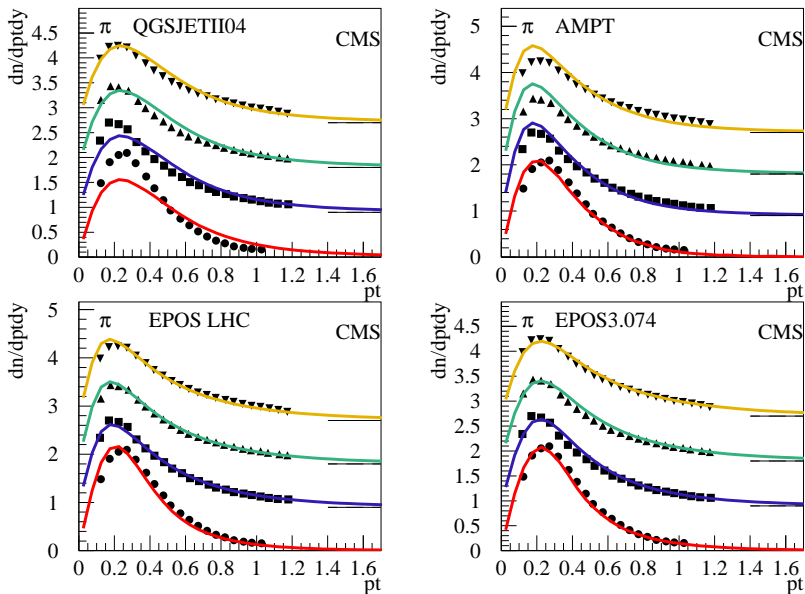
CMS: Multiplicity dependence of pion, kaon, proton pt spectra

CMS, arXiv:1307.3442

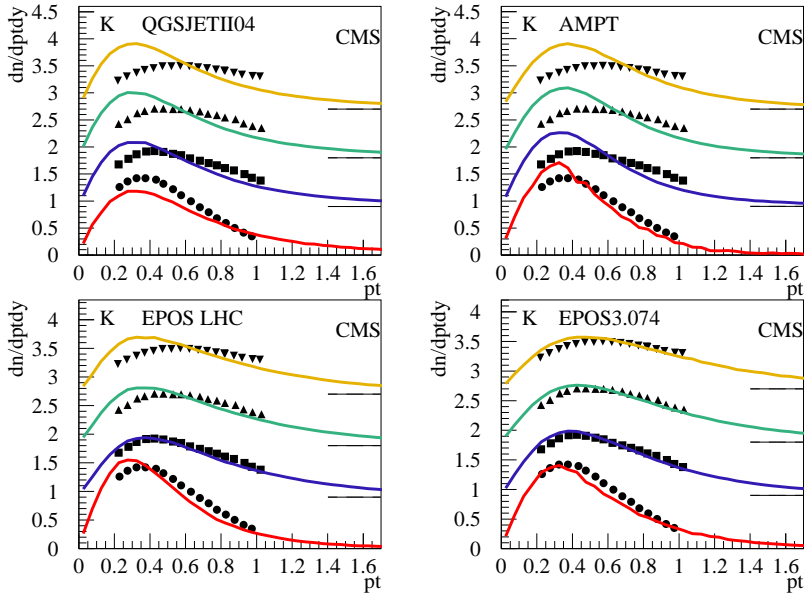
We plot 4 centrality classes:

$$\langle N_{\text{trk}}^{\text{offline}} \rangle = 8, 84, 160, 235 \text{ (in } |\eta| < 2.4)$$

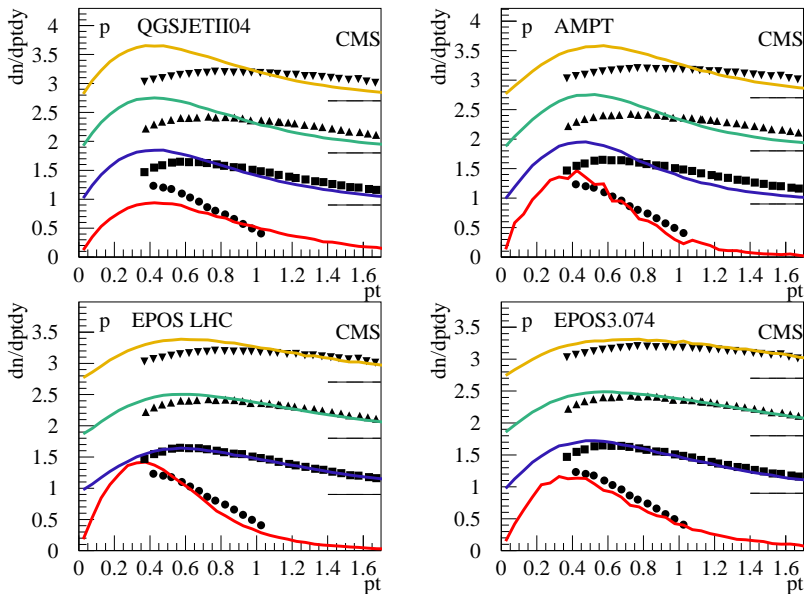
Multiplicity = centrality measure



Little change with multiplicity for pions



Kaon spectra change with multiplicity

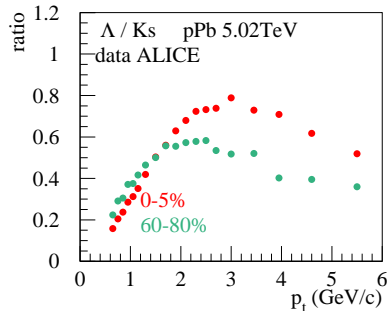
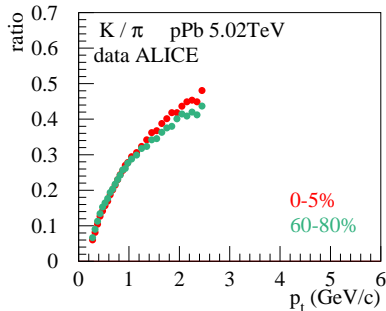


Strong variation of proton spectra => flow helps

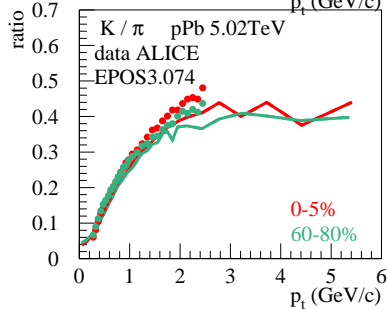
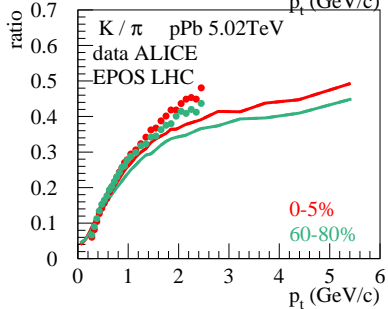
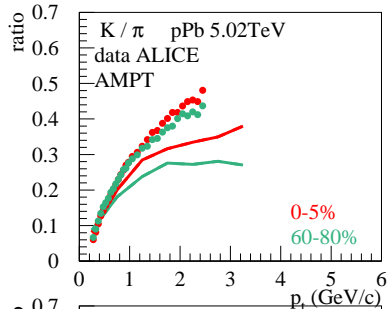
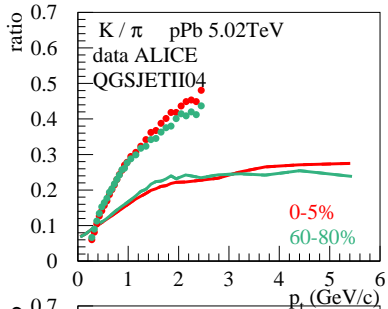
ALICE: compare pt spectra for identified particles in different multiplicity classes: 0-5%,...,60-80%

(in $2.8 < \eta_{\text{lab}} < 5.1$) From R. Preghenella, ALICE, talk Trento workshop 2013

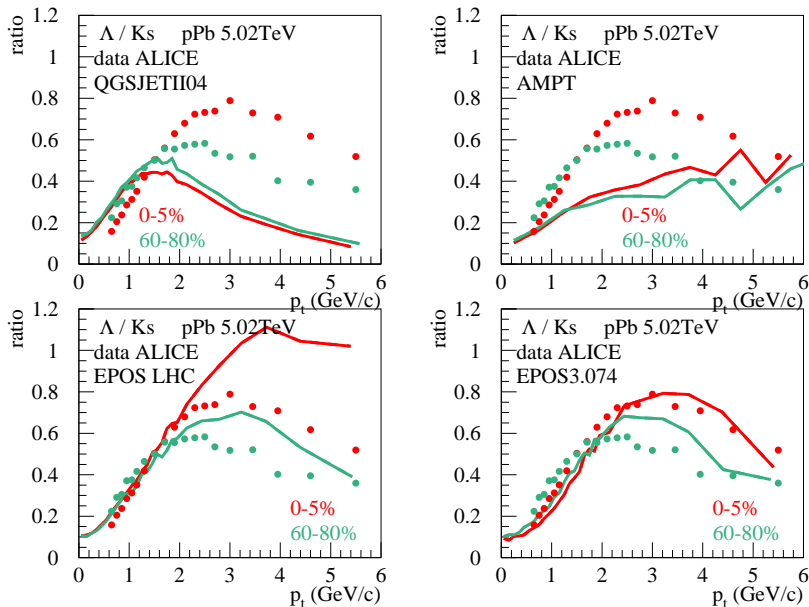
Useful : ratios (K/pi, p/pi...)



Significant variation of lambda/K – like in PbPb



No multiplicity dependence (not trivial to get the peripheral right)



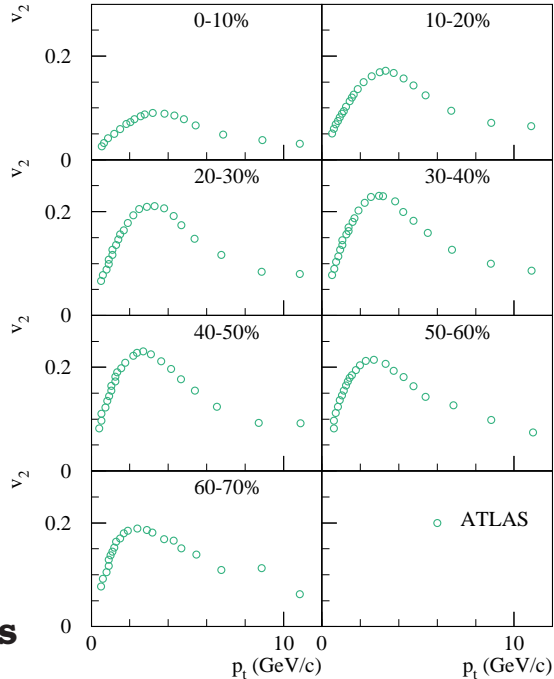
Significant multiplicity dependence. Flow helps

v_2 in PbPb

from central
to peripheral

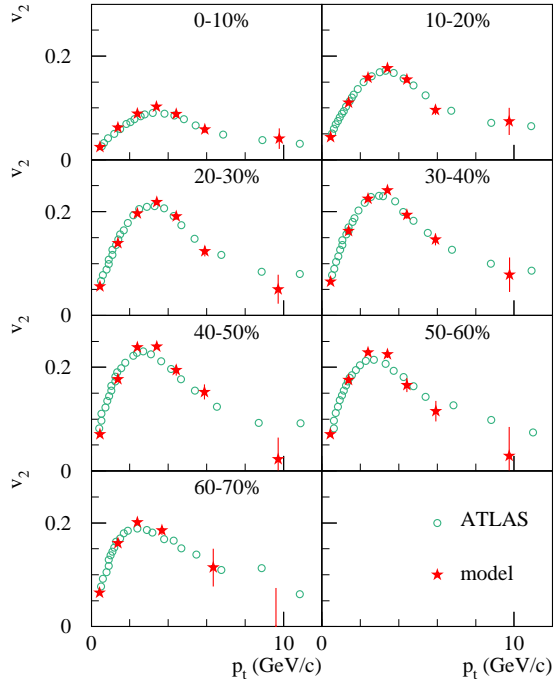
Changes
smoothly
towards
peripheral

=>
physics changes
smoothly



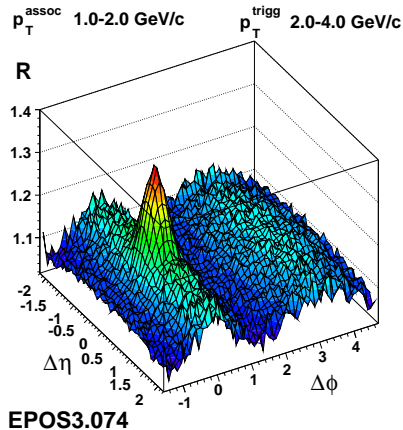
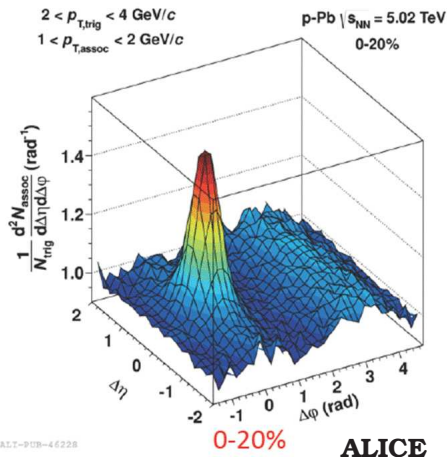
**with EPOS
simulations**

**Flow is
needed
even for
peripheral
collisions!**



“Ridges” in pA

ALICE, arXiv:1212.2001, arXiv:1307.3237



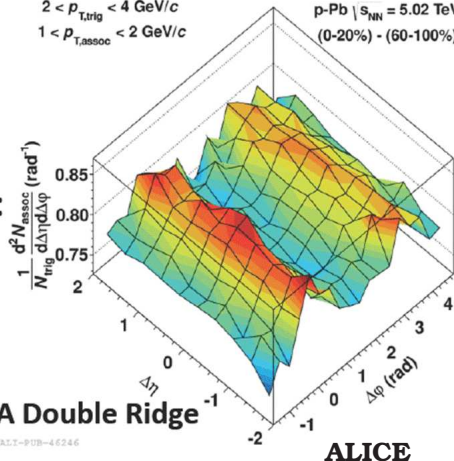
Central - peripheral (to get rid of jets)

$$2 < p_{T, \text{trig}} < 4 \text{ GeV}/c$$

$$1 < p_{T, \text{assoc}} < 2 \text{ GeV}/c$$

$$p\text{-Pb} \mid s_{NN} = 5.02 \text{ TeV}$$

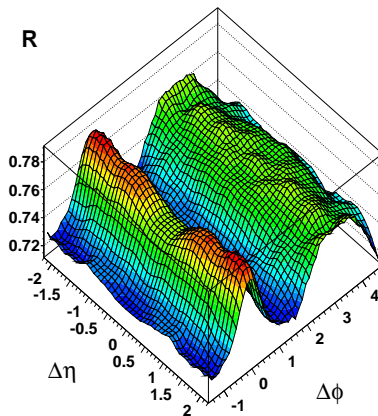
$$(0\text{-}20\%) - (60\text{-}100\%)$$



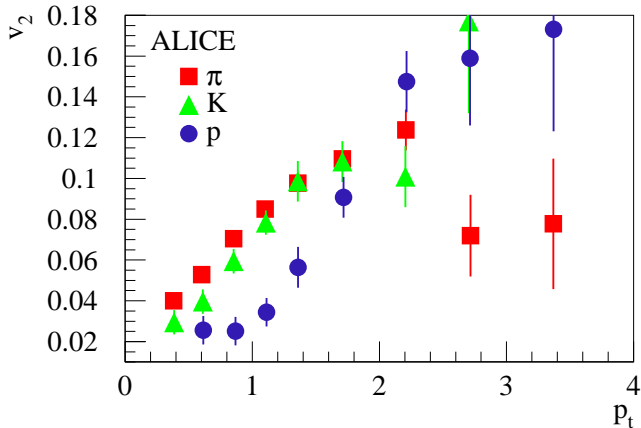
$$p_{T, \text{assoc}}^{\text{assoc}} \quad 1.0\text{-}2.0 \text{ GeV}/c$$

$$p_{T, \text{trig}}^{\text{trig}} \quad 2.0\text{-}4.0 \text{ GeV}/c$$

R



Identified particle v_2



mass splitting, as in PbPb !!!

pPb in EPOS3:

Pomerons (number and positions)
characterize geometry (P. number \propto multiplicity)

random

azimuthal

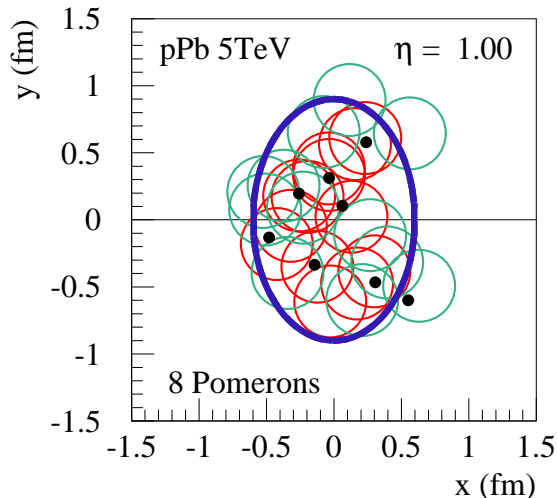
asymmetry

=>

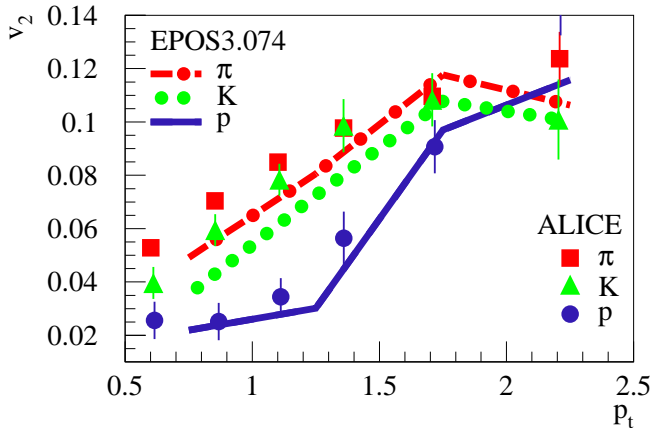
asymmetric flow

seen at higher pt

for heavier ptls



v_2 for π , K, p clearly differ



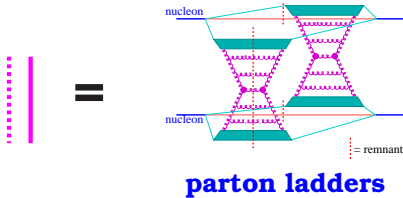
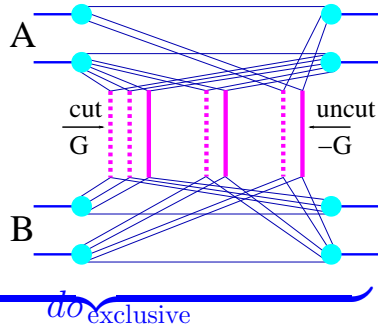
mass splitting, due to flow

VII Recent developments

**(Saturation, strangeness and
charm enhancement with
multiplicity)**

Reminder :

$$\sigma^{\text{tot}} = \sum_{\text{cut } P} \int \sum_{\text{uncut } P} \int$$



=> kinky strings

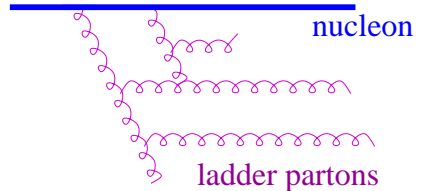


Non-linear effects

Computing the expressions G for single Pomeron:
A cutoff Q_0 is needed (for the DGLAP integrals).

**Taking Q_0 constant leads to a power law increase
of cross sections vs energy (=> wrong)**

**because non-linear effects
like gluon fusion are not
taken into account**



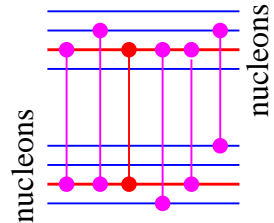
Solution: Instead of a constant Q_0 , use a dynamical **saturation scale for each Pomeron:**

$$Q_s = Q_s(N_{\text{IP}}, s_{\text{IP}})$$

with

N_{IP} = **number of Pomerons connected to a given Pomeron** (whose probability distribution depends on Q_s)

s_{IP} = **energy of considered Pomeron**



We get $Q_s(N_{\text{IP}}, s_{\text{IP}})$ from fitting

- the energy dependence of elementary quantities ($\sigma_{\text{tot}}, \sigma_{\text{el}}, \sigma_{\text{SD}}, dn^{\text{ch}}/d\eta(0)$) for pp
- the multiplicity dependence of dn^π/dp_t at large p_t for pp at 7 TeV

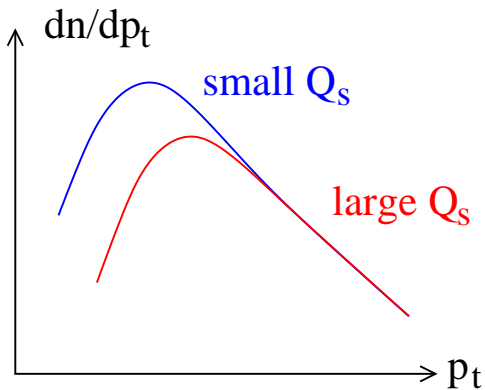
We find

$$Q_s \propto \sqrt{N_{\text{IP}}} \times (s_{\text{IP}})^{0.30}$$

CGC for AA:

$$Q_s \propto N_{\text{part}} \times (1/x)^{0.30}$$

Parton distributions



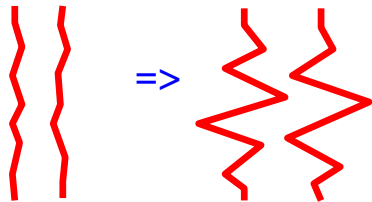
Increasing multiplicity

=> increasing N_{Pom}

=> Increasing Q_s

=> harder Pomerons

=> harder strings



=> more high p_t particles

=> Strong increase of $\langle p_t \rangle$ with multiplicity

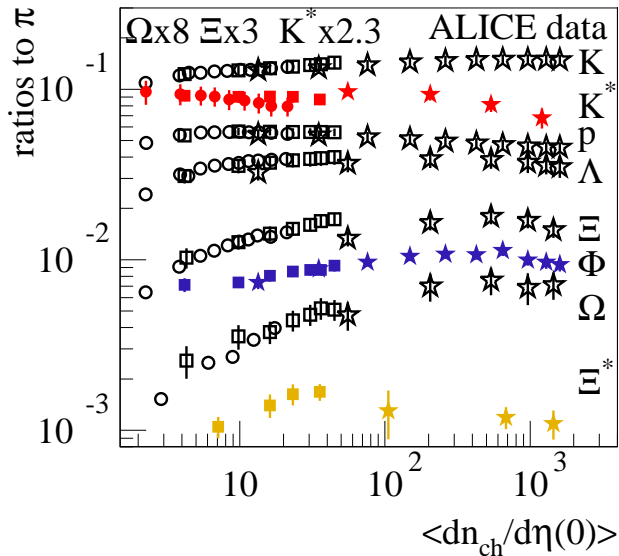
These saturation effects concern the corona !

What about multiplicity dependence of
core-corona separation ?

- **First check particle ratios**
(core-corona)
- **Then mean pt vs multiplicity**
(core-corona+saturation)

We compare simulations to ALICE data

Particle ratios to pions vs $\left\langle \frac{dn_{ch}}{d\eta}(0) \right\rangle$



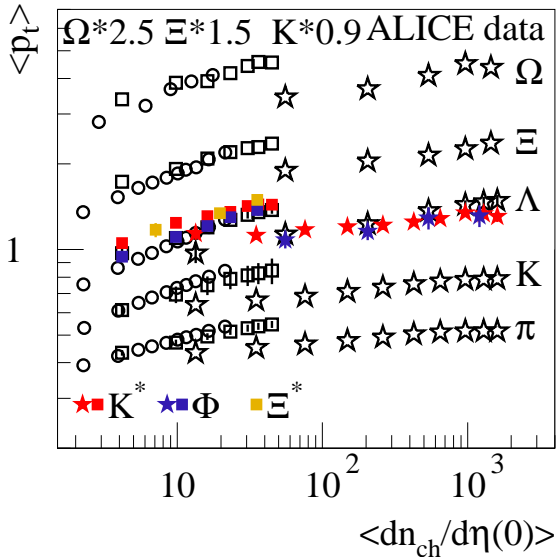
circles = pp (7TeV)

squares = pPb (5TeV)

stars = PbPb (2.76TeV)

Refs: next slide

Mean p_t vs $\left\langle \frac{dn_{ch}}{d\eta}(0) \right\rangle$



circles = pp (7TeV)

squares = pPb (5TeV)

stars = PbPb (2.76TeV)

Data partly collected by A. G. Knospe

Refs:

$\langle dn_{ch}/d\eta \rangle$ in Pb+Pb: Phys. Rev. Lett. 106 032301 (2011)
 π^+ , K^+ , and (anti)protons in Pb+Pb: Phys. Rev. C 88 044910 (2013)

Lambda in Pb+Pb: Phys. Rev. Lett. 111 222301 (2013)

Ξ^- and Omega in p+Pb: Phys. Lett. B 758 389-401 (2016)

π^+ , K^+ , (anti)protons, and Lambda in p+Pb: Phys. Lett. B 728 25-38 (2014)

$\langle dn_{ch}/d\eta \rangle$ in p+Pb: Eur. Phys. J. C 76 245 (2016)

Ξ^- and Omega in p+Pb: Phys. Lett. B 758 389-401 (2016)

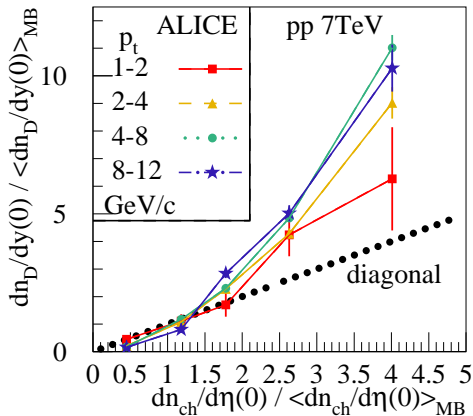
$\langle dn_{ch}/d\eta \rangle$ in p+p 7 TeV: Eur. Phys. J. C 68 345-354 (2010)

π^+ , K^+ , and (anti)protons in p+p 7 TeV: Eur. Phys. J. C 75 226 (2015)

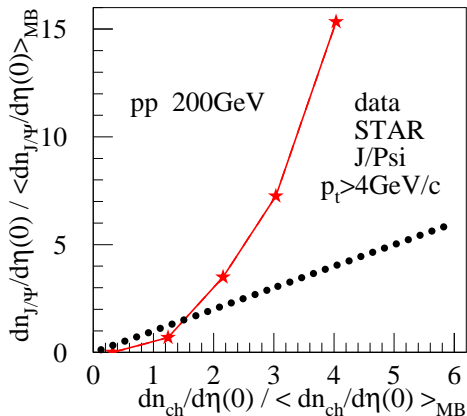
Ξ^- and Omega in p+p 7 TeV: Phys. Lett. B 712 309 (2012)

and data points from Rafael Derradi de Souza, SQM2016

D or J/ Ψ multiplicity vs $\frac{dn_{ch}}{d\eta}(0)$ in pp



ALICE JHEP 09 (2015) 148,
arXiv:1505.00664v1

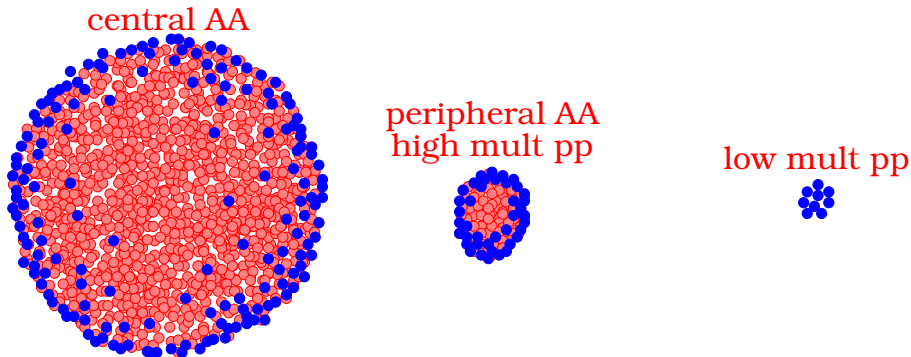


STAR, shown at MPI2016

strongly nonlinear increase

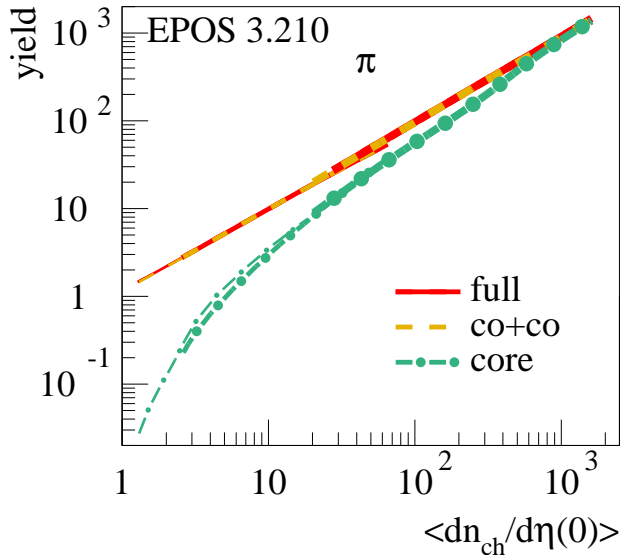
Core-corona picture in EPOS

Gribov-Regge approach => (Many) kinky strings
=> core/corona separation (based on string segments)



core => hydro => statistical decay ($\mu = 0$)
corona => string decay

Pion yields: core / corona contribution

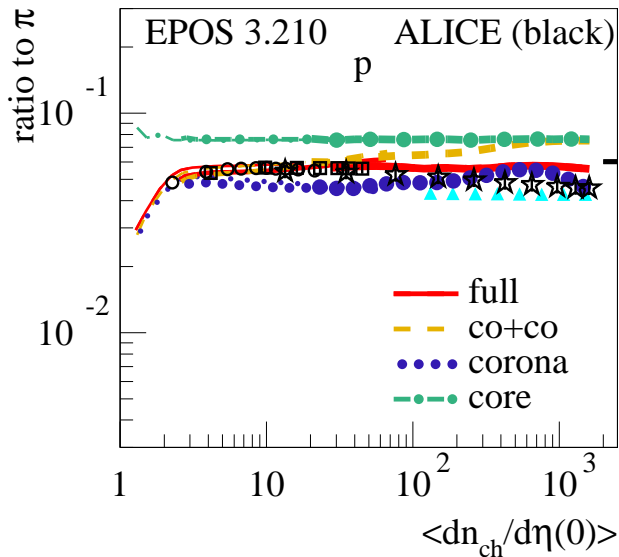


thick lines
= pp (7TeV)

thin lines
= pPb (5TeV)

hc = hadronic cascade
(UrQMD)

Proton to pion ratio



core hadronization:

$T = 164 \text{ MeV}, \mu_B = 0$

statistical model fit

(horizontal black line)

A. Andronic et al.,

arXiv:1611.01347

$T = 156.5 \text{ MeV}, \mu_B = 0.7 \text{ MeV}$

thick lines = pp (7TeV)

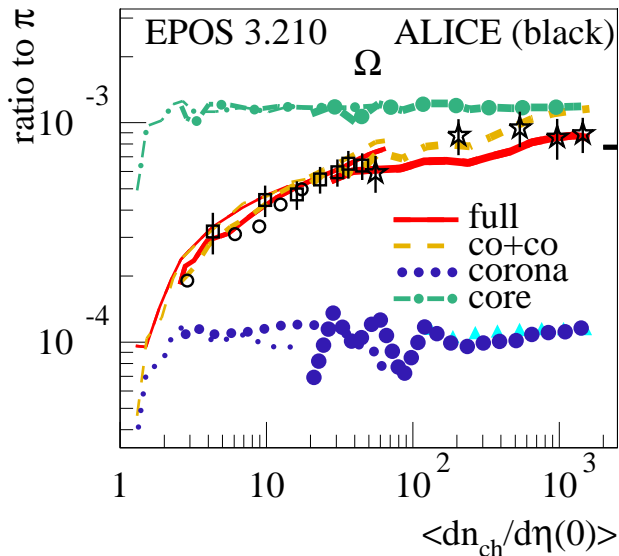
thin lines = pPb (5TeV)

circles = pp (7TeV)

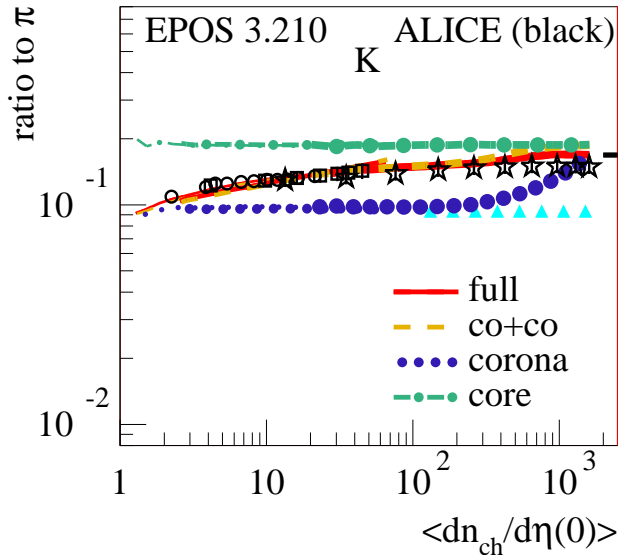
squares = pPb (5TeV)

stars = PbPb (2.76TeV)

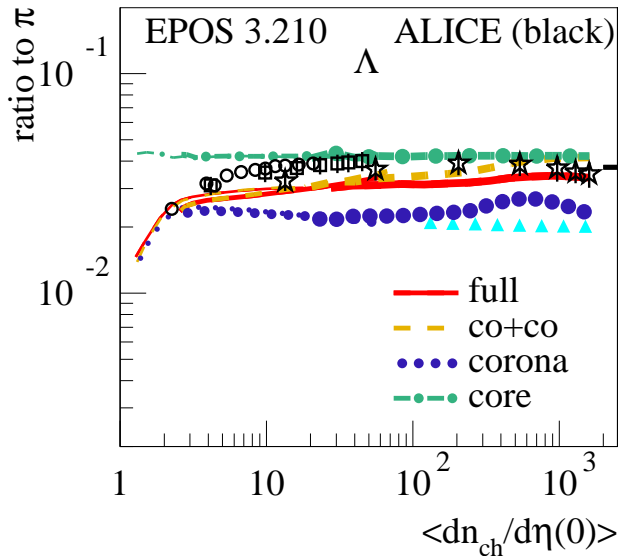
Omega to pion ratio



Kaon to pion ratio

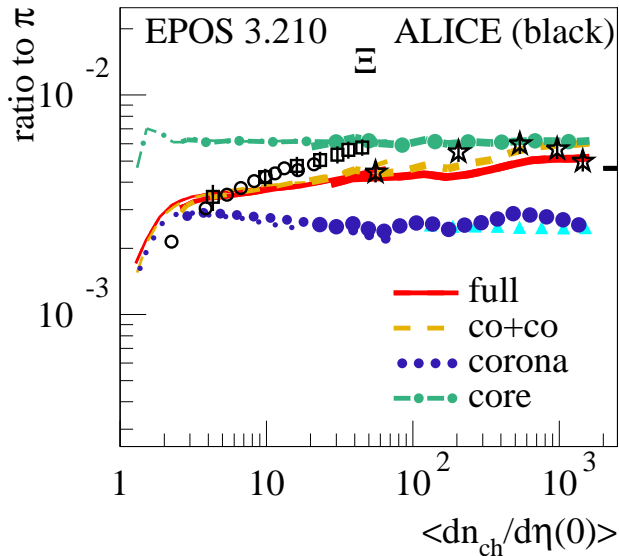


Lambda to pion ratio



thick lines = pp (7TeV)
 thin lines = pPb (5TeV)
 circles = pp (7TeV)
 squares = pPb (5TeV)
 stars = PbPb (2.76TeV)

Xi to pion ratio



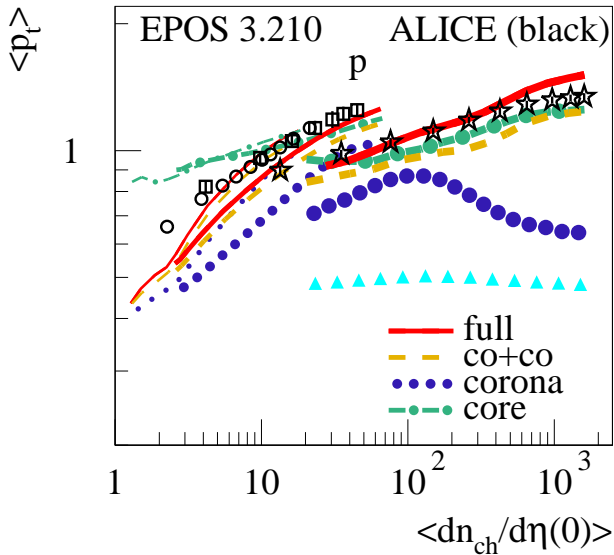
Ratios h/π for $h = p, K, \Lambda, \Xi, \Omega$ vs $\left\langle \frac{dn}{d\eta}(0) \right\rangle$:

Core and corona contributions separately roughly constant

Difference (core - corona) increasing for $p \rightarrow K \rightarrow \Lambda \rightarrow \Xi \rightarrow \Omega$

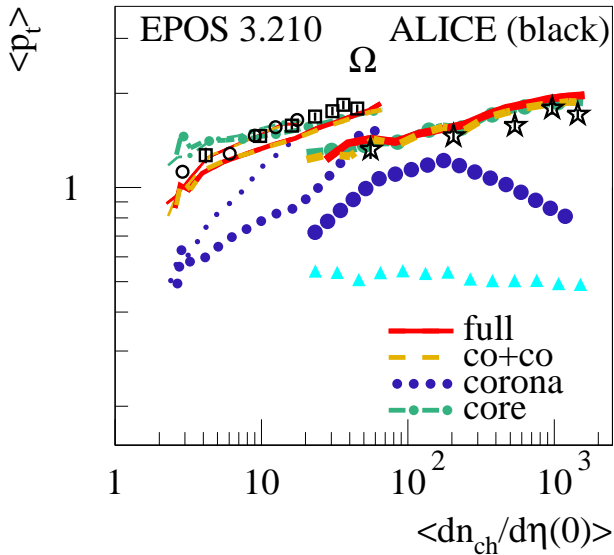
**=> increasing slope
(not enough for Ξ, Ω)**

Average p_t of protons



thin lines = pp (7TeV)
 intermediate lines = pPb (5TeV)
 thick lines = PbPb (2.76TeVV)
 circles = pp (7TeV)
 squares = pPb (5TeV)
 stars = PbPb (2.76TeV)

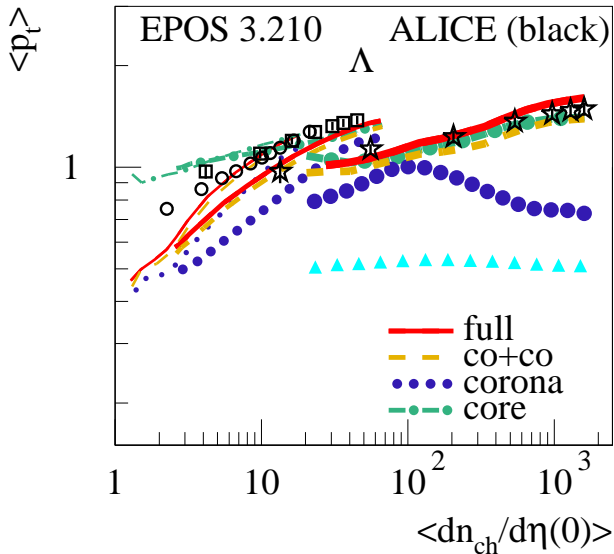
Average p_t of Omegas



thin lines = pp (7TeV)
 intermediate lines = pPb (5TeV)
 thick lines = PbPb (2.76TeVV)

circles = pp (7TeV)
 squares = pPb (5TeV)
 stars = PbPb (2.76TeV)

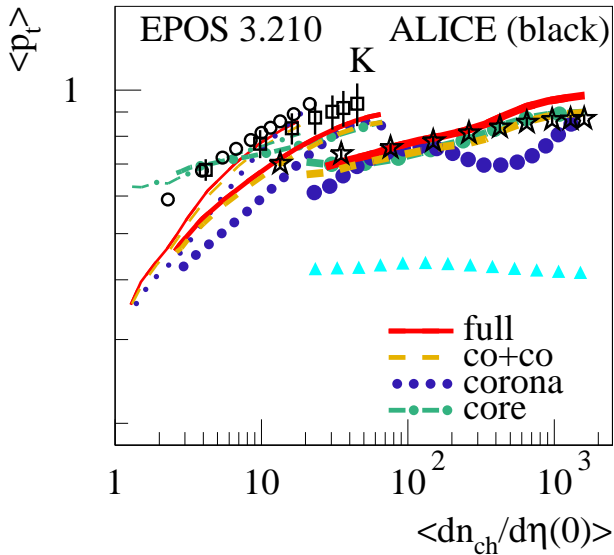
Average p_t of lambdas



thin lines = pp (7TeV)
 intermediate lines = pPb (5TeV)
 thick lines = PbPb (2.76TeVV)

circles = pp (7TeV)
 squares = pPb (5TeV)
 stars = PbPb (2.76TeV)

Average p_t of kaons



thin lines = pp (7TeV)
 intermediate lines = pPb (5TeV)
 thick lines = PbPb (2.76TeVVVV)
 circles = pp (7TeV)
 squares = pPb (5TeV)
 stars = PbPb (2.76TeV)

Average p_t of $K, p, \Lambda, \Xi, \Omega$ vs $\left\langle \frac{dn}{d\eta} \right\rangle_{(0)}$:

Moderate increase of core contribution
(same for pp and pPb, similar to PbPb)

Strong increase of corona contribution
(stronger for pp than for pPb, much stronger than for PbPb)

Slope(pp) > slope(pPb) >> slope(PbPb)

K, π : pp-pPb splitting

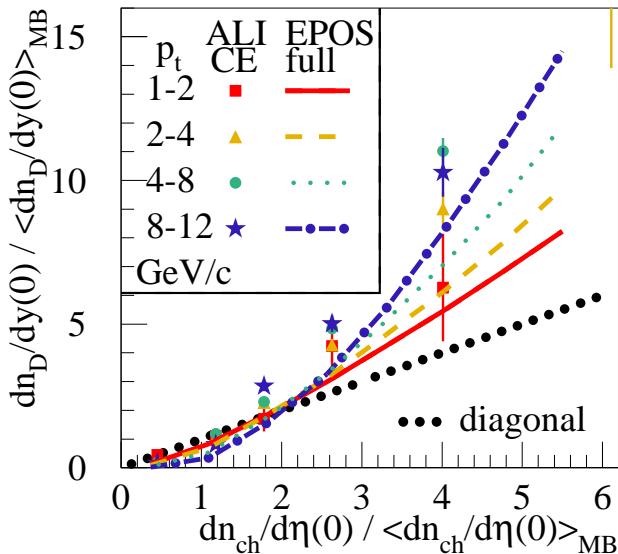
The multiplicity dependence of the corona contribution is crucial

Very closely related to this discussion:

**The multiplicity dependence
of charm production (D, J/ Ψ ,...)**

**The “ultimate tool” to test multiple
scattering (and the implementation
of Q_S)**

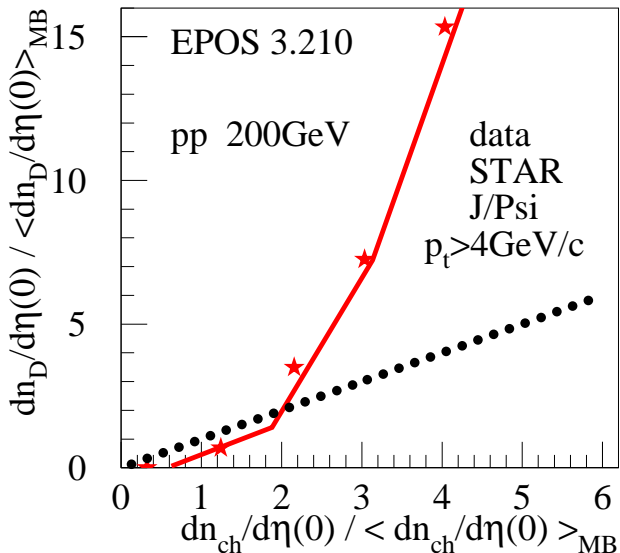
EPOS 3 compared to ALICE data



hadronic cascade
on/off
has no effect

hydro on/off
has small effect

EPOS 3 compared to RHIC data

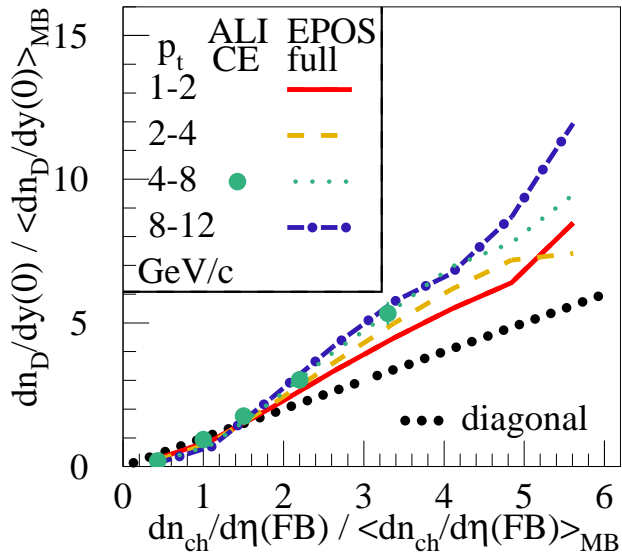


Calculations:
D mesons

Data: J/ Ψ

**Increase
stronger
than at LHC**

Multiplicity at FB rapidity (LHC)



**FB =
forward/backward
rapidity range:**

$$2.8 < \eta < 5.1$$

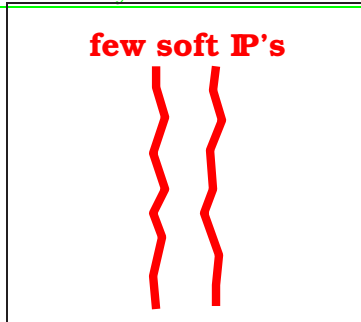
and

$$-3.7 < \eta < -1.7$$

Smaller increase

**Low
multi-
plicity
(LM)**

**Small
 N_{Pom}**



IP = Pomeron

**“Hardness”
increases
with N_{Pom}**

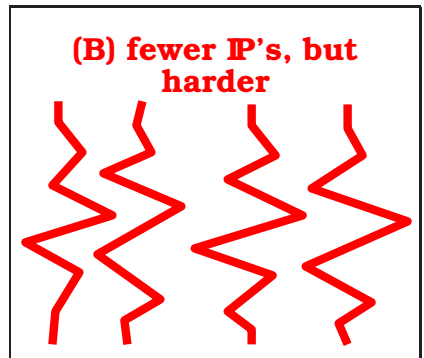
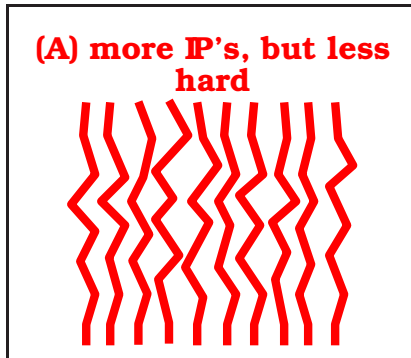
(larger Q_s)

**High
multi-
plicity
(HM)**

many

hard

**IP's
on avg**



LM → HM:

Pomerons get harder (larger Q_s)

→ favors high pt or large masse production

**in particular due to case B (fewer IP's, but harder)
for highest pt bins !**

**Bigger effect at RHIC due to much narrower N_{Pom}
distribution (harder IP's are needed)**

Smaller effect for $\frac{dn}{d\eta}(FB)$ as multipl. variable

**(case B is replaced by case C: fewer IP's, but more covering
the FB rapidity range)**